NTIA TM-90-145

PROCEDURE FOR CALCULATING THE POWER DENSITY OF A PARABOLIC CIRCULAR REFLECTOR ANTENNA

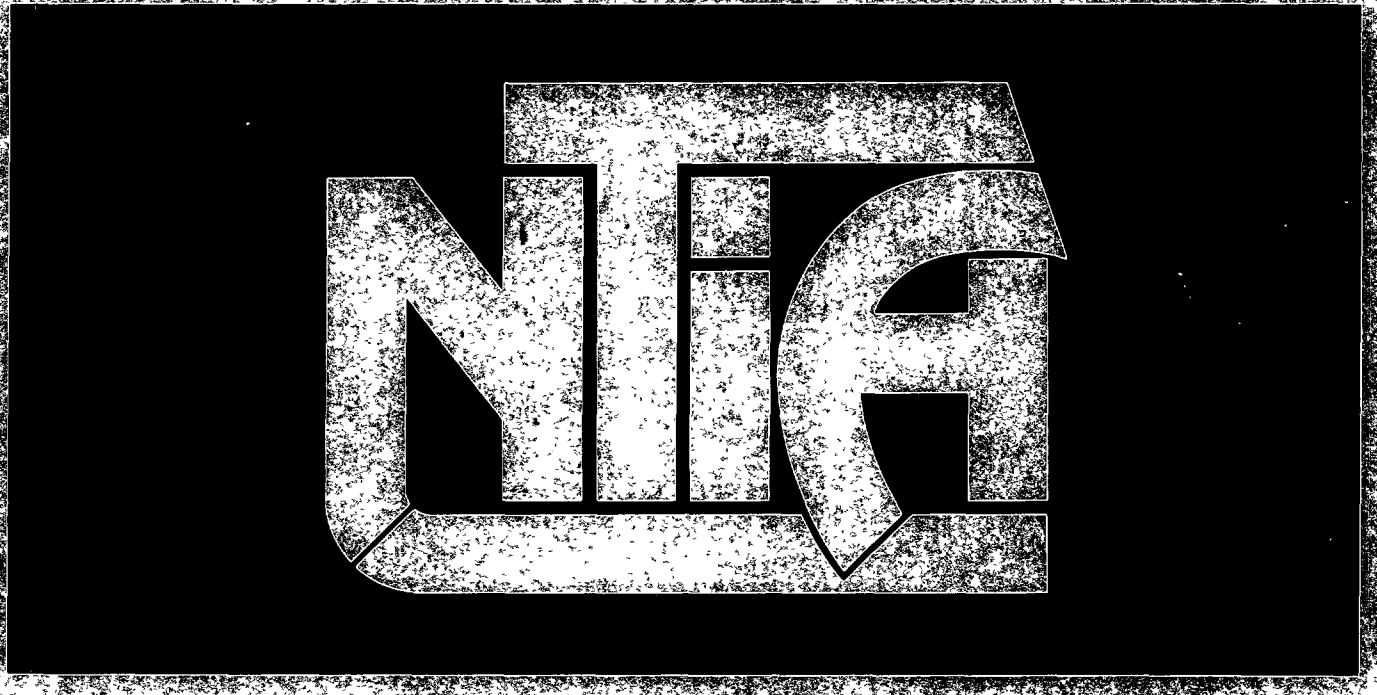

technical memorandum series

U.S. DEPARTMENT OF COMMERCE • National Telecommunications and Information Administration

NTIA TM-90-145

PROCEDURE FOR CALCULATING THE POWER DENSITY OF A PARABOLIC CIRCULAR REFLECTOR ANTENNA

Herbert K. Kobayashi

U.S. DEPARTMENT OF COMMERCE
Robert A. Mosbacher, Secretary

Janice Obuchowski, Assistant Secretary
for Communications and Information

FEBRUARY 1990

ABSTRACT

This technical report details a procedure for calculating the mainbeam off-axis power density in the near- and far-field of a parabolic circular reflector antenna. In this report, the on-axis procedures of NTIA TM-87-129 and its IBM-PC compatible Antenna Field Intensity (AFI) program are extended to off-axis analysis. Like its predecessors, it is intended for general use in system planning and evaluation and gives a worst-case estimate for radiation hazard assessment.

The procedure starts with the on-axis power density at a given distance obtained from the TM-87-129 report or AFI PC program. This is multiplied by the normalized near-field power density for the chosen off-axis angle to give a final answer.

The simple log-function form of the normalized curves lends itself to inclusion in the automated AFI program as a computer algorithm.

The method chosen for developing the procedure is general and may be applied to other directive antennas provided sufficient near-field off-axis data are available.

KEYWORDS

Antenna Field Intensity (AFI) Program

Near-Field Off-axis Power Density

On-axis Field Intensity

Parabolic Reflector (Circular)

TABLE OF CONTENTS

SECTION 1

INTRODUCTION

SECTION 2

SUMMARY AND RECOMMENDATIONS

SECTION 3

PARABOLIC CIRCULAR APERTURE ANALYSIS

TABLE OF CONTENTS
(Continued)

SECTION 4

APPENDIX

REFERENCES

LIST OF TABLES

TABLE

TABLE OF CONTENTS
(Continued)

LIST OF FIGURES

FIGURE

TABLE OF CONTENTS
(Continued)

LIST OF FIGURES

SECTION 1

INTRODUCTION

BACKGROUND

The National Telecommunications and Information Administration (NTIA) is responsible for managing the Federal Government's use of the radio frequency spectrum. NTIA's responsibilities include establishing policies concerning spectrum assignment, allocation and use, and providing the various departments and agencies with guidance to ensure that their conduct of telecommunications activities is consistent with these policies.[1]

This report and its NTIA predecessors TM-87-129 and TM-88-135 address the need for simple, easy-to-use procedures to estimate the near-field power density of common transmitting antennas and compliance with the national radiation criteria.[2,3,4]

From the earlier reports, the near-field power density along the axis of the mainlobe can be calculated for common linear (wire) and aperture antennas. The off-axis power density could only be found for directional wire antennas, although general procedures using numerical computational codes and applicable to most antennas were outlined.

The manual calculations required by the procedures were automated in the IBM PC-compatible AFI (Antenna Field Intensity) program, now in its second version, AFI2.[5]

---

[1] NTIA, *Manual of Regulations and Procedures for Federal Radio Frequency Management*, U.S. Department of Commerce, National Telecommunications and Information Administration, Washington, D.C., Revised May 1989.

[2] Farrar, A. and Chang E., *Procedures for Calculating Field Intensities of Antennas*, NTIA Report TM-87-129, U.S. Department of Commmerce, September 1987.

[3] Kobayashi, H. K., *Procedures for Calculating Field Intensities of Antennas: Phase II*, NTIA Report TM-88-135, U.S. Department of Commerce, September 1988.

[4] American National Standards Institute, *Safety Levels with Respect to Human Exposure to Radio Frequency Electromagnetic Fields, 300 kHz to 100 GHz*, Report No. ANSI C95.1-1982, Institute of Electrical and Electronic Engineers, Inc., New York, NY, 1982.

[5] Calhoon, E. and Kobayashi, H. K., *Documentation for the Antenna Field Intensity Program Version 2 (AFI2)*, NTIA/CSD, Annapolis, MD.

OBJECTIVES

The specific objectives of this report were to:

1. follow the recommendations in NTIA Report TM-88-135 by extending the off-axis near-field coverage of antenna types by providing a simple procedure for the important parabolic circular aperture antenna, and

2. provide the data from which algorithms can be developed for inclusion of the procedure into the AFI PC-IBM compatible program series.

APPROACH

To accomplish the aforementioned objectives, the following approach was taken.

1. The literature, including Federal agency technical reports, was consulted for mainlobe off-axis publications on the dish antenna.

2. The literature findings were consolidated, verified by numerical computation, and transformed into normalized parametric curves of near-field power density versus mainlobe off-axis angle.

SECTION 2

CONCLUSIONS AND RECOMMENDATIONS

INTRODUCTION

This report addresses the need of NTIA and other government agencies for evaluation of the off-axis field intensity of particular antennas for the system review process and radiation hazard assessment. In continuing the trend of developing simple procedures requiring easily available input data, the parabolic circular reflector antenna is treated as an isolated system and the effect of support structures, such as feed struts, are not considered.

CONCLUSIONS

The objectives of this report listed in Section 1 have been met as follows:

1. A simple procedure was developed for calculating the near-field off-axis field intensity of the circular parabolic reflector antenna in terms of readily available input data.

2. The procedure followed the approach taken in recent NTIA publications on the on-axis field calculation of generic antenna types, and is similar in its application.

3. Automation of the procedure was ensured by the development of normalized parametric data curves easily translatable into log-function algorithms for incorporation in the AFI2 IBM-PC compatible program.

RECOMMENDATIONS

The following are NTIA staff recommendations based on the technical findings contained in this report. NTIA management will evaluate these recommendations to determine if they can, or should, be implemented from a policy, regulatory, or procedural viewpoint. Any action to implement these recommendations will be accomplished under separate correspondence by modification of established rules, regulations, or procedures. It is recommended that the following be done by NTIA.

1. The procedure in this report should be used by NTIA when calculating the near-field off-axis intensities of circular parabolic reflector antennas.

2. The normalized power density curves developed in this report should be the basis for an automated procedure in a new version of the AFI IBM-PC compatible program.

3. The feasibility of producing near-field off-axis calculation procedures for other directive antennas and arrays should be continued on a case-by-case basis and documented as necessary.

SECTION 3

PARABOLIC CIRCULAR APERTURE ANALYSIS

INTRODUCTION

Aperture antennas have been known to be a potential source of harmful radiation to humans for at least 30 years because of their ability to strongly focus RF power.[6] Most operate in the VHF-to-SHF (> 200 MHz) range where the human body is at quasi-resonance with this class of non-ionizing radiation.[7] The most common aperture antennas employ a parabolic reflector. These comprise 18% of the 100,000 antennas in the Government Master File (Ref. 3, page 3-2). This report deals with the ubiquitous circular or dish-shaped parabolic reflector antenna whose on-axis behavior has been discussed in detail in Ref. 2, pages 4-9 to 4-19.

APERTURE DISTRIBUTION AND D/λ AS PARAMETERS

The relationship between the far-field radiation pattern of a parabolic dish antenna and the aperture distribution, dish diameter D, and the wavelength λ (elucidated in Silver 40 years ago) is still the starting point for gross near-field analyses today.[8] Silver showed that if an aperture distribution $F(\rho)$ of the following form is assumed

$$F(\rho) = [1 - (2\rho/D)^2]^n \qquad 0 < \rho < D/2 \qquad (3\text{-}1)$$

where n = aperture taper

then n (not necessarily an integer) can be related to the ratio D/λ and certain radiation pattern characteristics as shown in TABLE 1.

---

[6] Mumford, W. W., *Some Technical Aspects of Microwave Radiation Hazards*, IRE (IEEE) Proceedings, Vol. 49, no. 2, pp. 427-447, February 1961.

[7] National Council on Radiation Protection and Measurements, *Biological Effects and Exposure Criteria for Radio Frequency Electromagnetic Fields*, page 274, NCRP Report No. 86, National Council on Radiation Protection and Measurements, Bethesda, MD, 1986.

[8] Silver, S. (Editor), *Microwave Antenna Theory and Design*, pages 192-195, McGraw-Hill, Inc., New York, NY, 1949.

TABLE 1

CIRCULAR APERTURE CHARACTERISTICS FROM SILVER
(see Ref. 8)

Taper n	Half-power beamwidth rad	Relative gain g	First Sidelobe below peak dB
0	1.02 λ/D	1.00	−17.6
1	1.27 λ/D	0.75	−24.6
2	1.47 λ/D	0.56	−3.7
3	1.65 λ/D	0.44	−36.1

We see that relative gain is traded for a lower first sidelobe and a broader beam as $F(\rho)$ of Equation 3-1 changes from a constant or uniform (n = 0) amplitude to one of extreme taper. In practice, a compromise is usually found between 1 and 2.[9] Sometimes a "pedestal" or constant b is added to Equation 3-1 as seen below

$$G(\rho) = b + [1-(2\rho/D)^2]^n \qquad 0 < \rho < D/2 \qquad (3\text{-}2)$$

in order to increase gain. The effect of b on the near-field sidelobes will be taken up later. The diagrams on the following page of $F(\rho)$ variation across the circular aperture give some idea of how aperture taper sharpens with increasing n:

---

[9] Bickmore, R. W. and Hansen, R. C., *Antenna Power Densities in the Fresnel Region*, IRE (IEEE) Proceedings, pp. 2119-2120, December 1959.

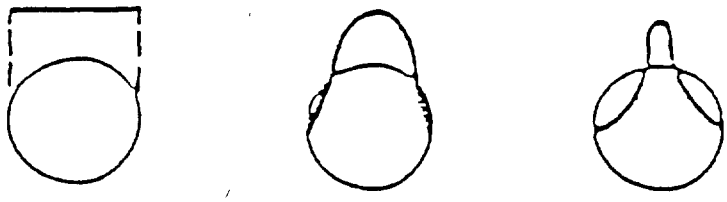

Figure 3-1. Circular aperture illumination as a function of n.[10]

For **on-axis** near-field calculations, Farrar and Adams (among others) also used n and D/λ as input parameters to closed-form integral expressions.[11] In the form of fast, efficient computer algorithms, these generated the "lookup" curves in Ref. 2 needed to manually calculate the actual on-axis power density. The curves are normalized to the power at the far-field distance d of

$$d = 2D^2/\lambda \qquad (3\text{-}3)$$

In the AFI PC program (Ref. 5), the equations are in the form of algorithms enabling all computations to be done automatically.

---

[10] Skolnik, M. I. (Editor), Radar Handbook, pages 9-20 to 9-24, McGraw-Hill, Inc., New York, NY, 1970. An excellent illustrated discussion on the trade-off between aperture shape and far-field parameters can be found here.

[11] Farrar, A. and A. T. Adams, *An Improved Model for Calculating the Near Field Power Densities of Aperture Antennas*, IEEE International Symposium on Electromagnetic Compatibility, pp. 134-137, 1980.

DEVELOPMENT OF A PROCEDURE FOR OFF-AXIS CALCULATIONS

Approach

The previous paragraphs have shown that the **on-axis** calculations depend on knowing the normalized near-field power density variation as a function of distance with n and D/λ as parameters. An **off-axis** procedure would include the on-axis calculation plus the effect of going off-axis in the near-field. Because of rotational symmetry, the average power density at one radial distance is completely expressed for a given pair of n and D/λ by a single function $f(\theta)$, where θ the off-axis angle ranges from 0 to 90 degrees. This simplicity is not realizable for other apertures, including ellipsoidal and square shapes.

The steps in developing a procedure for off-axis calculations are as follows:

1. Examine pertinent sources of near-field data and reduce them to a common form for ease in comparison.

2. Develop normalized power density curves relating antenna and near-field geometry from the comparisons.

3. Combine a near-field "correction" from the curves with the on-axis power density (previously found) in a simple algebraic sequence to give the desired off-axis power density.

Power density in the near-field

Three published sources will be compared starting from the simplest aperture distribution of n = 0 and a small D/λ of 10, and ending with a tapered pedestal distribution with D/λ greater than 30.[12,13,14] For ease in comparison, the data from each source will be converted into semi-log graphs of normalized power density versus off-axis angle with distance as a parameter.

---

[12] Lewis and Newell, *An Efficient and Accurate Method for Calculating and Representing Power Density in the Near-Zone of Microwave Antennas*, NBSIR 85-3036, December 1985.

[13] Hansen, R. C. and L. L. Bailin, *A New Method of Near Field Analysis*, IRE (IEEE) Transactions on Antennas and propagation, pp. S458-A467, December 1959.

[14] Maddocks, H. C. (Editor), *ECAC Antenna Engineering Handbook*, pages 5-65 to 5-74, IIT Research Institute, ECAC-HDBK-79-051, revised October 1985.

Source 1: Hansen and Bailin (see Ref. 13):

Hansen and Bailin were able to extend Silver's analysis and ".... make near-field calculations feasible for the first time" (see Ref. 8). The choice of a flat uniform distribution (n=0) enabled the solution to be expressed in terms of Hankel functions. For ease in computation, Hansen picked particular points for radial distance, the independent variable.

Figure 3-2, simplifed from Hansen, displays the E-field curves at three near-field distances normalized to the far-field distance at $2D^2/\lambda$ (see Equation 3-3). An additional curve at $2D^2/\lambda$ is included for comparison. Hansen normalized the E-field magnitude to the greatest value at the chosen distance.

A more conventional treatment of the curves in Figure 3-2 can be found in Figure 3-3. Off-axis angle is plotted on a log scale, thus emphasizing the angles near boresight. The E-field is converted to power density in dB and normalized to the on-axis value for the chosen distance (i.e. the zero dB level). Each curve is replaced by line segments drawn through the sidelobe maximas. This conforms to the usual far-field antenna pattern (distance = ∞); but in this case, for near-field patterns at chosen distances. As in the far-field case, the power density at any off-axis angle can be found by knowing the on-axis antenna gain. For the near-field, the on-axis gain can be obtained by manual calculations (see Ref. 2) or from a PC program (see Ref. 5).

Both Figures 3-2 and 3-3 show interesting trends. As distance is decreased, the sidelobes remain essentially unchanged from the point of entry into the near-field (solid line curve at $2D^2/\lambda$) until nearly 3/4 of the distance to the antenna is traversed. Then the mainlobe starts to bifurcate while the sidelobe envelope flattens perceptibly.

Following the method above for Source 1, **All data from Sources 2 and 3 will be reduced to the form of Figure 3-3 for comparative purposes.**

Source 2: ECAC Handbook: (See Ref. 14.)

The ECAC Engineering Handbook has curves for estimating the near-field power density for aperture distributions: n = 0, 1, 2, and 3. ECAC's curves cannot be directly compared to Hansen's because calculations involve parametric "dispersion" charts such as Figure 3-4. In these charts, the parameter $\bar{x}$ in the Figure relates power dispersion to geometry as follows

$$\bar{x} = 2Y/D \qquad \text{Eq. 5-40, Ref. 14} \qquad (3\text{-}4)$$

where: Y = off-axis distance
D = diameter of dish

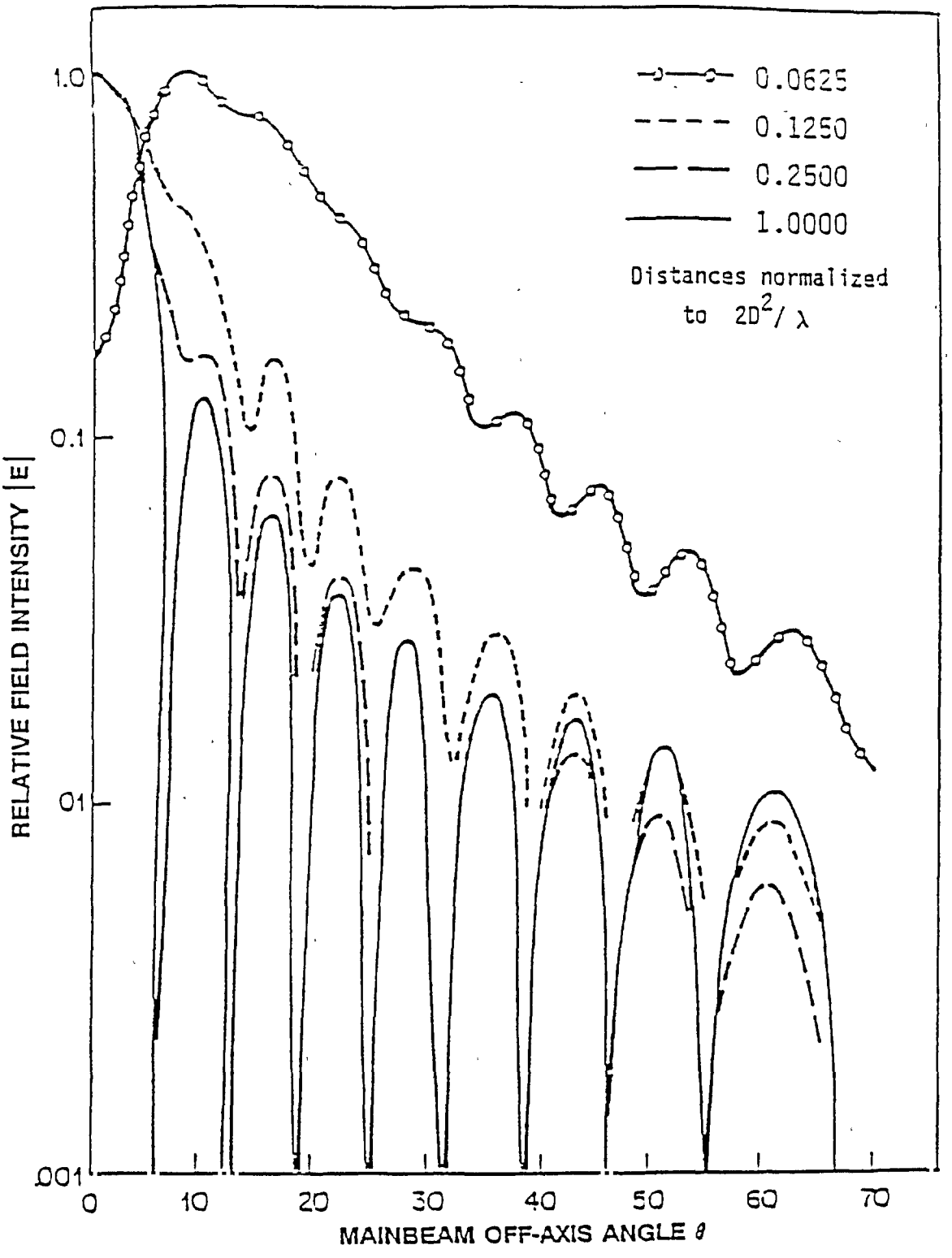

Figure 3-2. Relative field intensity vs mainbeam off-axis angle. n = 0, D = 10λ, simplified after Ref. 13.

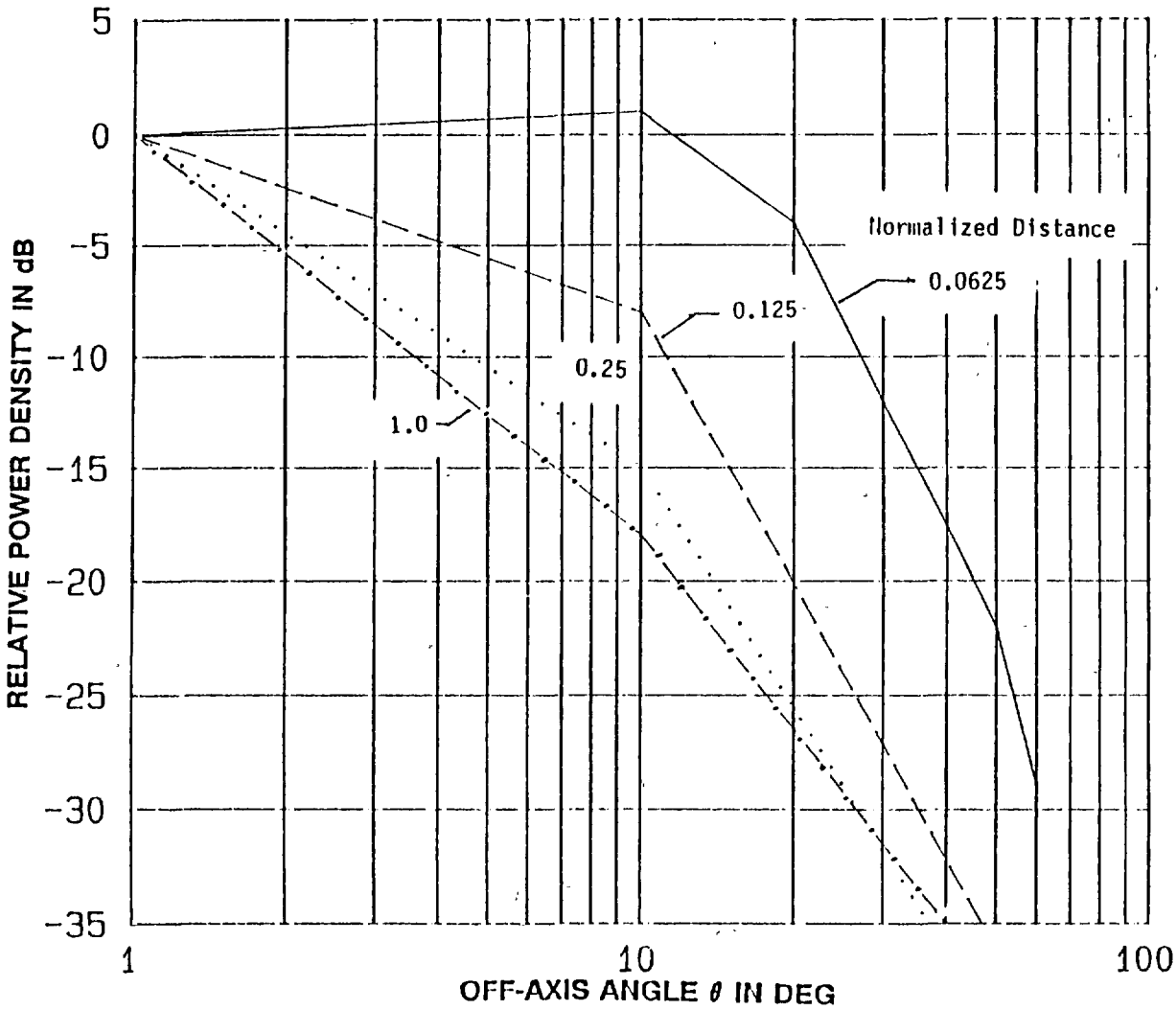

Figure 3-3. Relative power density versus off-axis angle. n = 0, D/λ = 10, based on data from Figure 3-2.

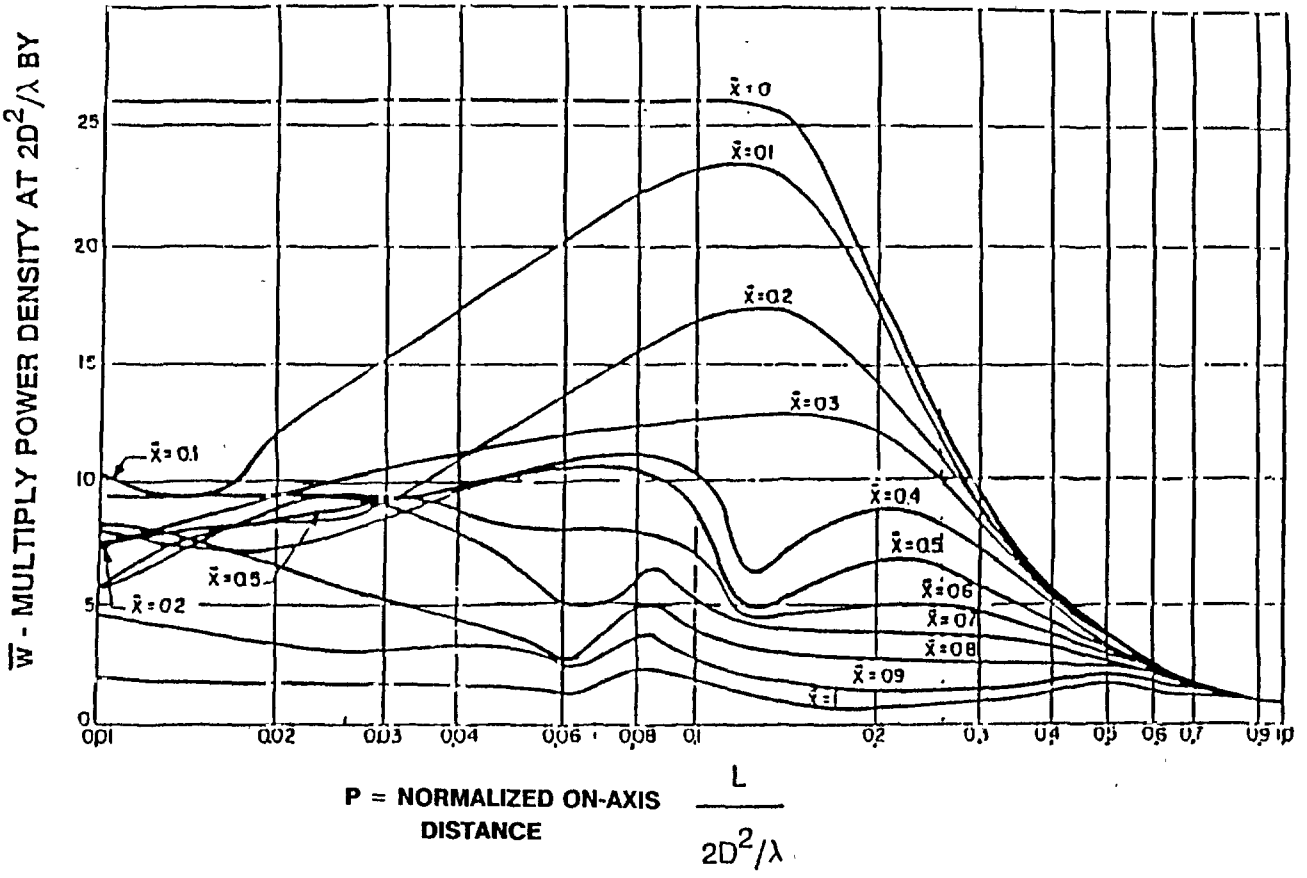

Figure 3-4. Power dispersion curves, n = 0.
Taken directly from Fig. 5-34, Ref. 14.

The normalized on-axis distance P of Figure 3-4 is related to geometry by

$$P = L/(2D^2/\lambda) \text{ Eq. 5-41, Ref. 14} \qquad (3\text{-}5)$$

where: L = on-axis distance from antenna
λ = wavelength of emission

By definition, the off-axis angle θ is

$$\theta = \arctan (Y/L) \qquad (3\text{-}6)$$

Solving Equations 3-4 and 3-5 for Y and L respectively and substituting into Equation 3-6, we get

$$\theta = \arctan [\lambda \bar{x}/(4DP)] \qquad (3\text{-}7)$$

Using the same $D/\lambda = 10$ ratio as Ref. 14, we get

$$\theta = \arctan (0.025 \bar{x}/P) \qquad (3\text{-}8)$$

For a given distance L, a normalized distance P can be found by Equation 3-5. Each intersection of P with a $\bar{x}$ curve will yield an off-axis angle and a correction factor.

For example, let L = 2.5 m and D = 1.0 m. Substituting into Equation 3-5,

$$P = L/(2D^2/\lambda) = 2.5/[2(1.0)(10)] = 0.125$$

At the intersection of x = 0.4 and P = 0.125, the normalized power density = 7. The off-axis angle can be found from Equation 3-8:

$$\theta = \arctan [0.025\ x/P) = \arctan [0.025(0.4)/0.125$$

$$= 4.57 \text{ degrees}$$

The steps above have been repeated for the same normalized distances as in Hansen and Bailin for n = 0, 1, 2 and 3. The results are plotted on semi-log scale in Figures 3-5a to 3-5d.

Source 3: Lewis and Newell (see Ref. 12):

Lewis and Newell (NBS, Boulder, CO) devised a stable, efficient means of numerically integrating the plane-wave spectrum representation of the near-zone and Fresnel region. Figure 3-6 taken directly from their report is a cartesian plot of Y-distance versus the Z or on-axis distance normalized to D^2/λ for n = 2 and D/λ = 10. To transform their data, an expression for power density as a function of the off-axis angle was developed as follows.

1. The z-axis distance is normalized to $2D^2/\lambda$.

2. The off-axis angle θ is found by the definition

$$\theta = \arctan (y/z) \qquad (3\text{-}9)$$

where: $y = YD$ from the ordinate, Figure 3-6 (3-10)

and: $z = Z(2D^2/\lambda)$ (3-11)

Substituting into Equation 3-9, we get

$$\theta = \arctan [0.5Y\lambda/(ZD)] \qquad (3\text{-}12)$$

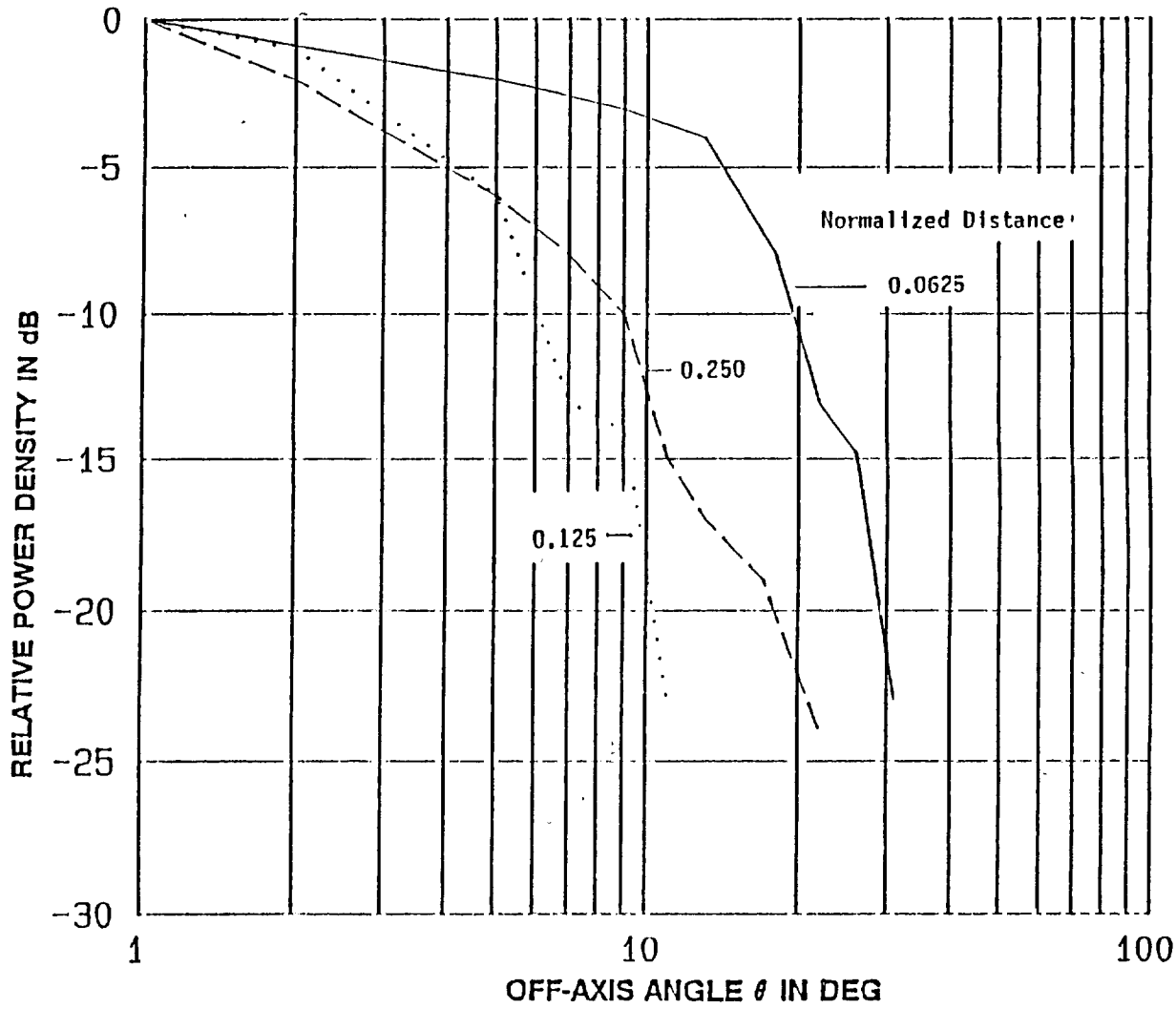

Figure 3-5a. Relative power density vs mainbeam off-axis angle. n = 0, D = 10λ, based on data from Ref. 14.

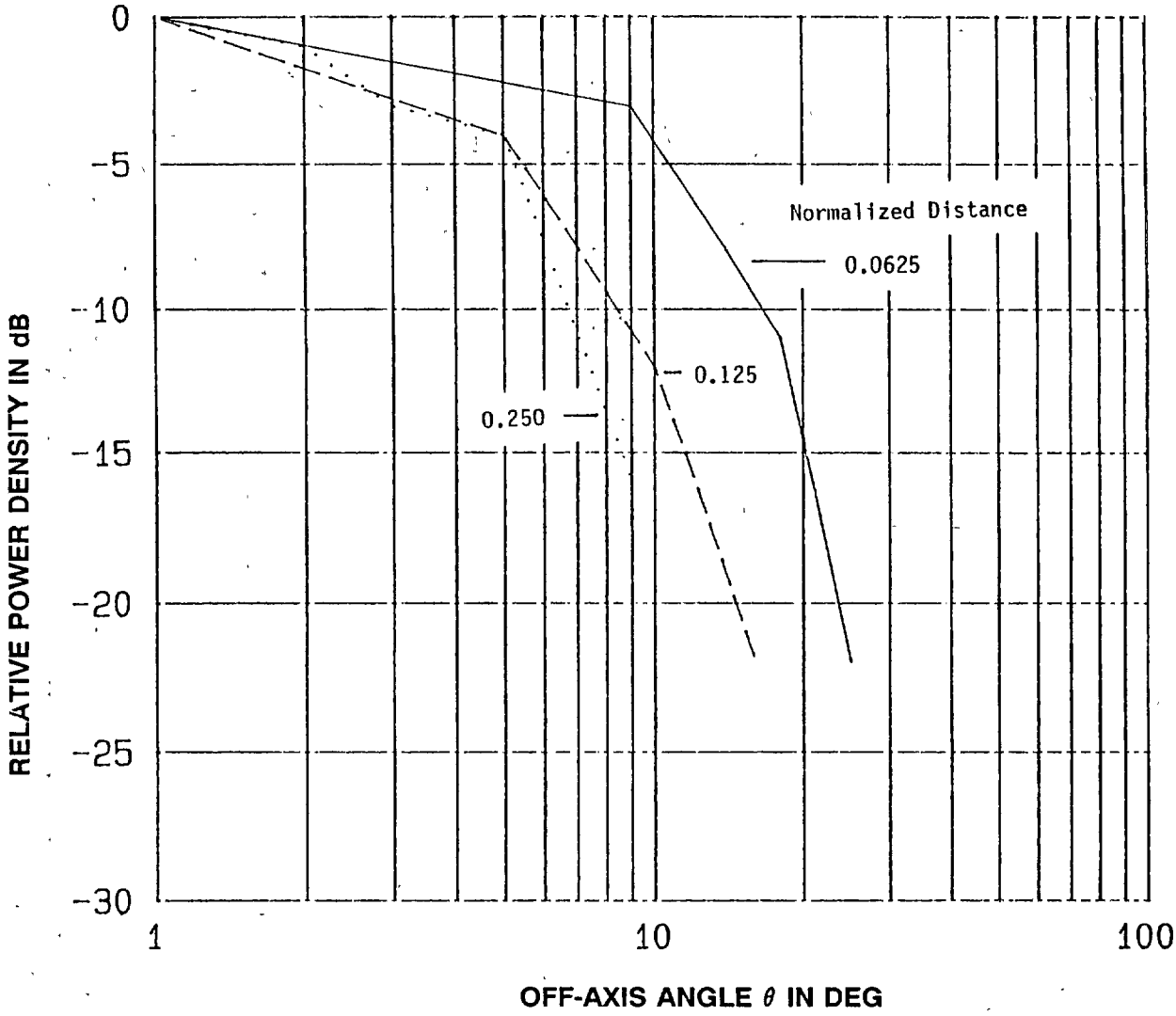

Figure 3-5b. Relative power density vs mainbeam off-axis angle. n = 1, D = 10λ, based on data from Ref. 14.

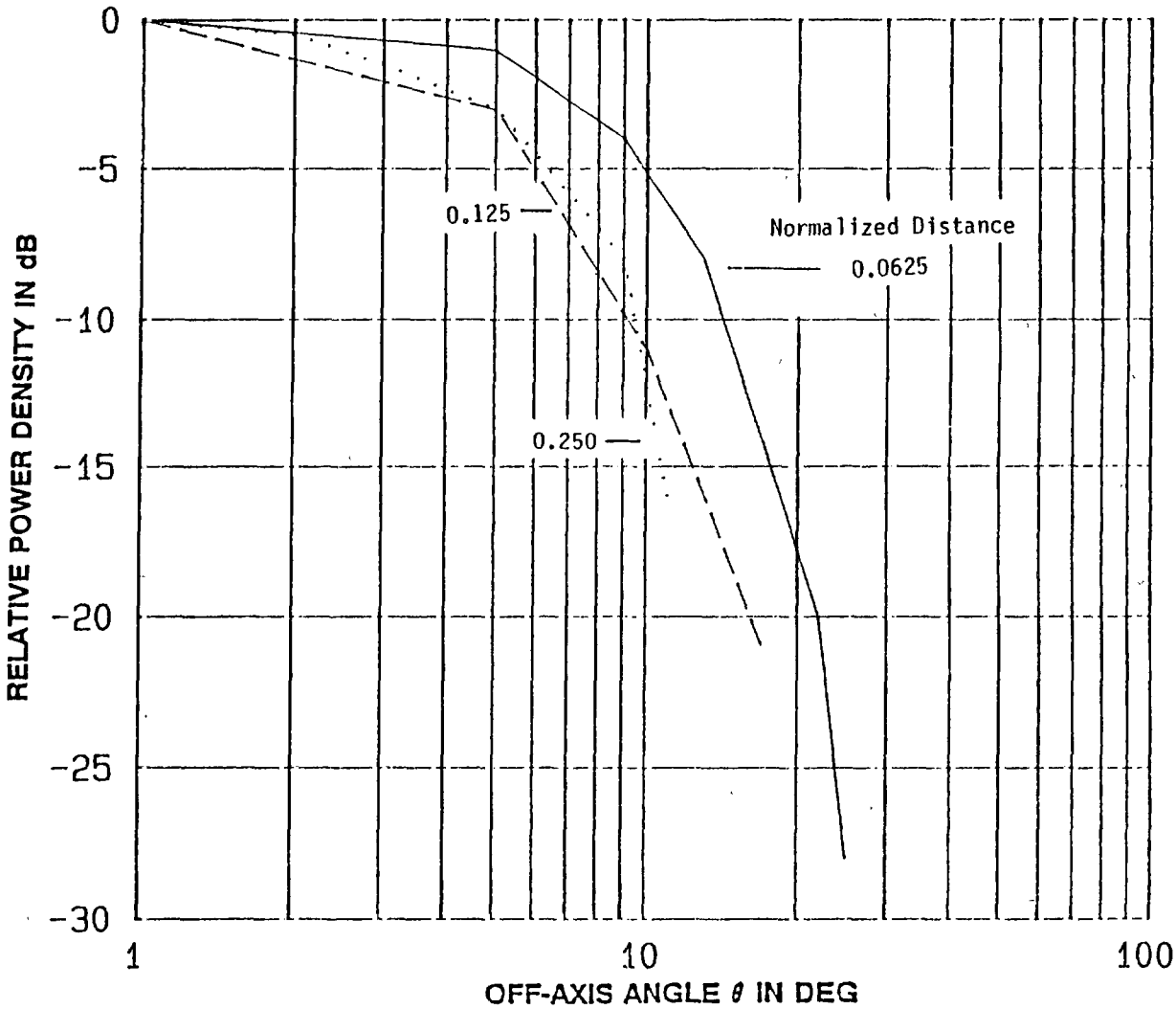

Figure 3-5c. Relative power density vs mainbeam off-axis angle. n = 2, D = 10λ, based on data from Ref. 14.

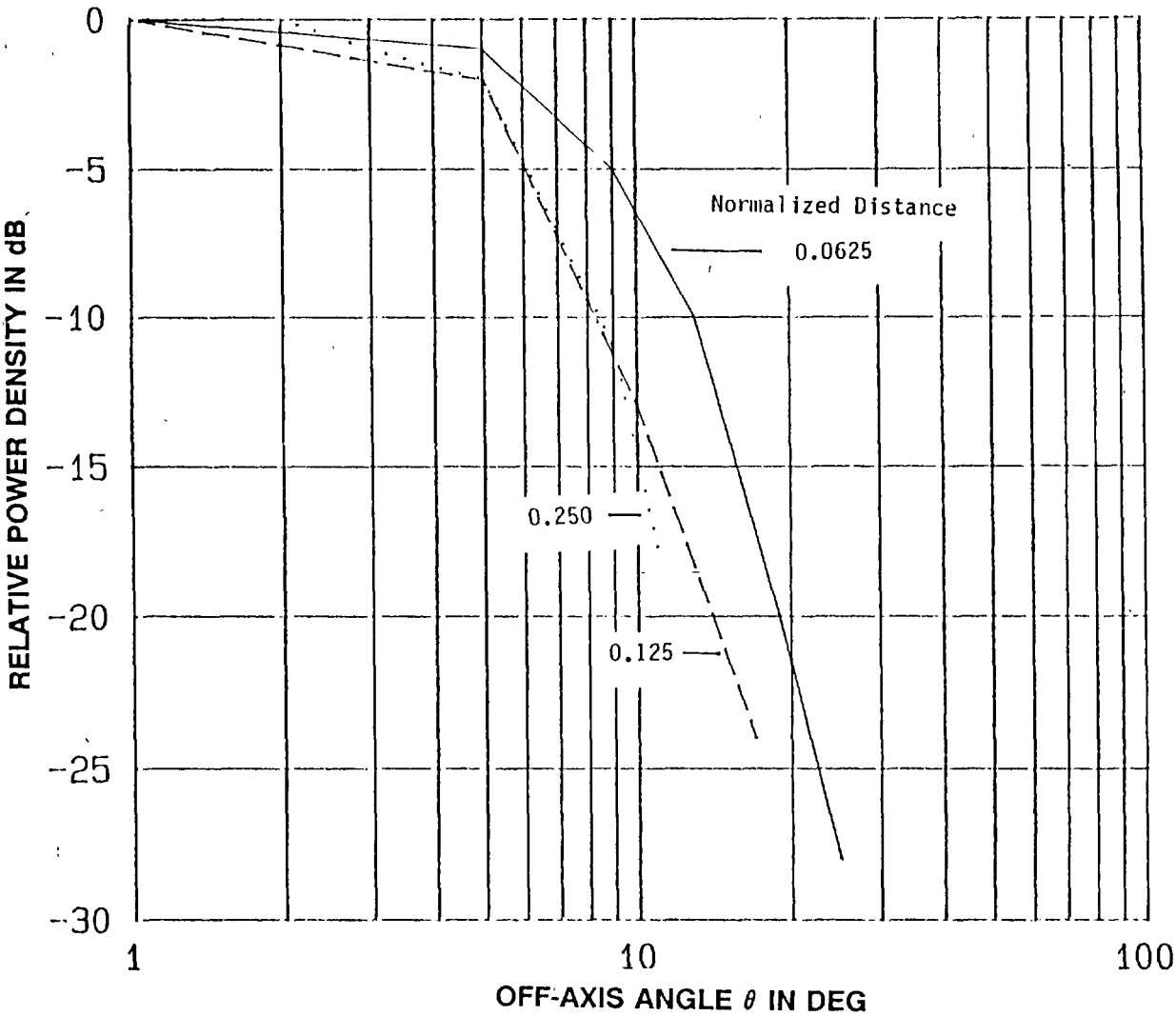

Figure 3-5d. Relative power density vs mainbeam off-axis angle. n = 3, D = 10λ, based on data from Ref. 14.

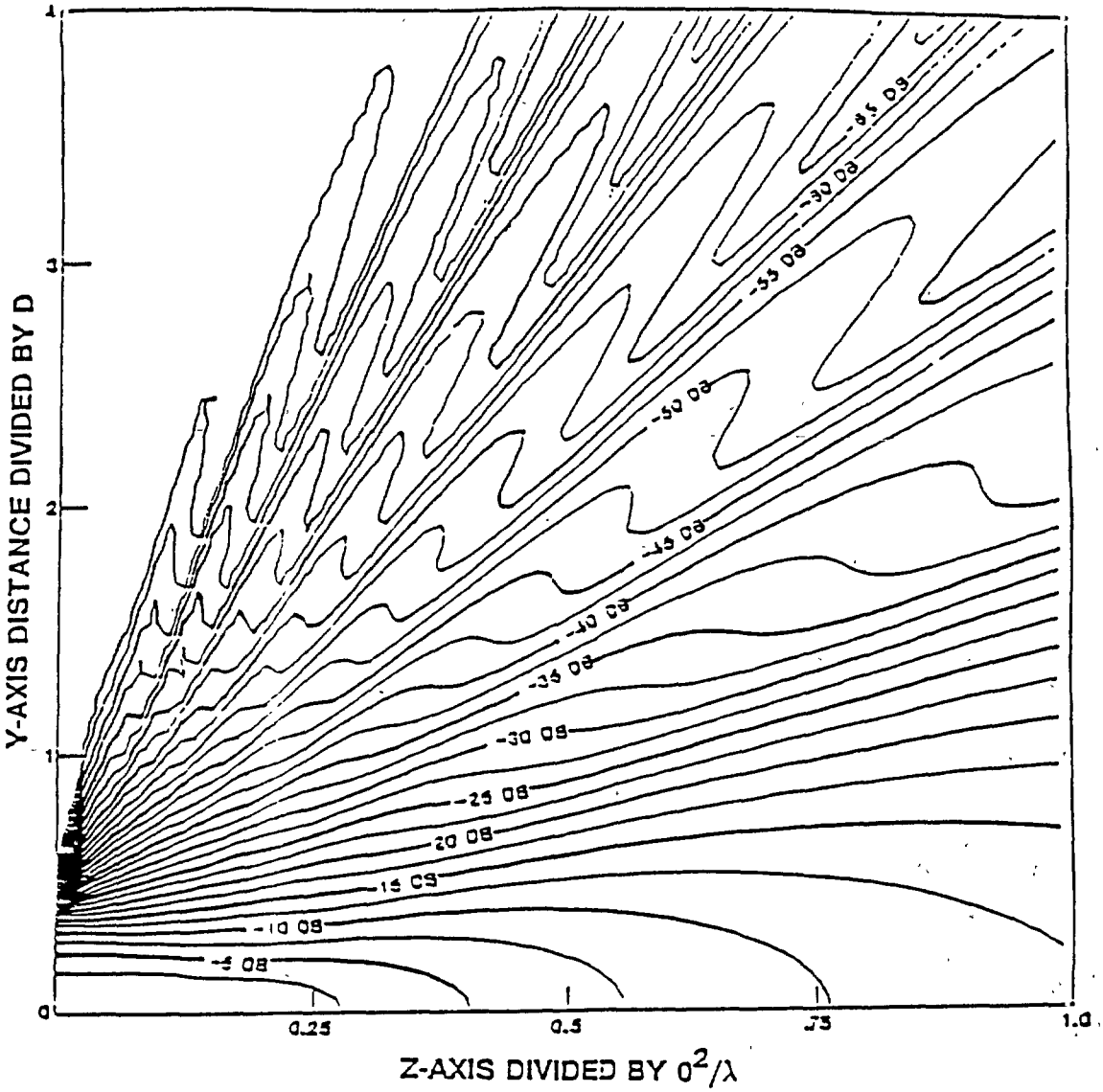

Figure 3-6. Relative power density curves in the Y - Z plane. n = 2, D = 10λ, taken directly from Fig. 6, Ref. 13.

Using the same $D/\lambda = 10$ ratio as Refs. 13 and 14,

$$\theta = \arctan(0.05Y/Z) \qquad (3\text{-}13)$$

For given distance y and z, normalized Y and Z can be found from Equations 3-10 and 3-11 and substituted into Equation 3-13 to get the off-axis angle.

3. Relative power density corresponding to the off-axis angle θ can be read from Figure 3-6.

The procedure just described was repeated for the same normalized distances in Hansen, and the results plotted in Figure 3-7 (see Ref. 13).

Small-Aperture Near-Field Power Density:

The power density in the near-field of a small-aperture dish ($D/\lambda = 10$) for the three sources can now be compared from Figures 3-3, 3-5a-d, and 3-7. Some general observations are:

1. The slope of a curve around boresight ($\theta = 0$) tends to flatten out as the distance is shortened.

2. Away from boresight at any given distance, the slope tends to steepen as the aperture taper becomes sharper, i.e., n increases.

As discussed earlier, the normalized power density itself need not be considered here since it can be related at any time to the on-axis power density obtained from Refs. 2 or 5.

Effect of Larger Dish Sizes and Aperture Pedestals:

Lewis and Newell (see Ref. 12) found that the density contours of Figure 3-6 changed smoothly as D/λ was increased until no change occurred at and above the ratio of 30. This invariant condition holds if y and z (see Equation 3-9) do not exceed 4D and D^2/λ, respectively.

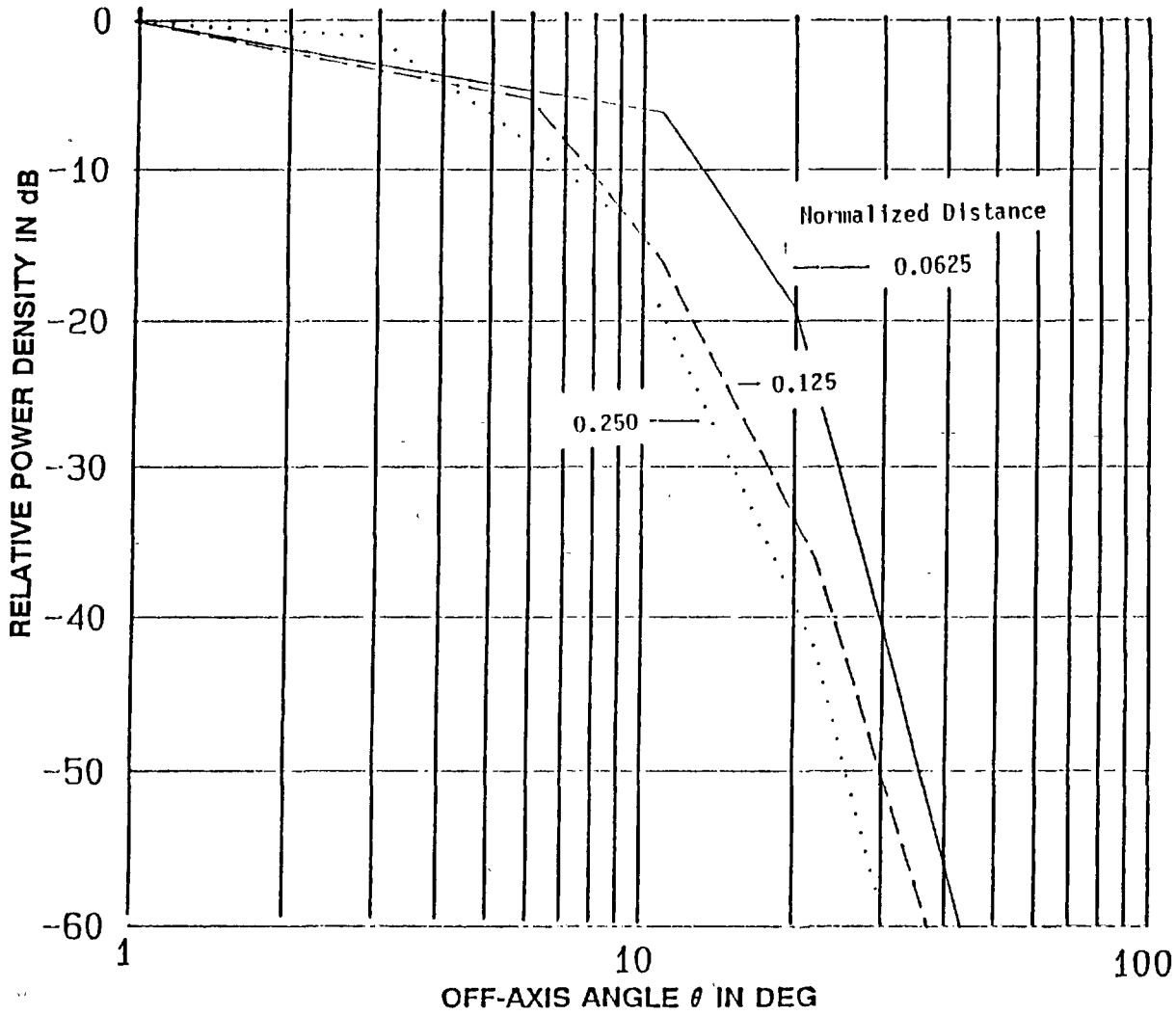

Figure 3-7. Relative power density vs mainbeam off-axis angle. n = 2, D = 10λ, based on data from **Ref. 13.**

The power density slopes at $D/\lambda = 30$ were plotted (Figure 3-8a) and found to be similar to those at $D/\lambda = 10$ (Figure 3-7) at angles away from boresight. Note that a graph of $D/\lambda > 30$ cannot be made because the off-axis angle (computed from Equation 3-12) depends on a specified D/λ ratio here chosen to be 30.

A pedestal added to the aperture distribution (Equation 3-2) usually steepens the slope and adds "destructive interference" (*ibid* p. 4) at larger angles. This phenomenon appears in Figure 3-8b for a –20 dB (b = 0.1) pedestal where the slope is slightly steeper than in the no-pedestal case (Figure 3-8a) and the curves cannot be extended past the angle of invariance. Curves for a –10 dB pedestal, b = 0.316 (not shown here) had similar results.

Power density curves for $D/\lambda = 30$ (Figures 3-9a through 3-9d) calculated from charts in the ECAC Handbook agree with Lewis and Newell. In particular, slopes compare well at all distances for n = 2 (Figures 3-8a and 3-9c). As anticipated, large and small dishes both show the same progression to steeper slopes with increasing aperture taper (cf 3-5a, 3-5b and 3-9a, 3-9b).

Derivation of Relative Power Curves of the Procedure:

In the previous pages, curves have been developed for showing trends in power density in terms of antenna parameters and near-field geometry. Because the curves conform closely to straight-line segments when plotted on a semi-log scale, simple analytic expressions could easily replace them.

But in order to avoid manual computational errors involving logarithms, analytical expressions will not be part of this procedure and will be deferred for inclusion in the Antenna Field Intensity (AFI) IBM-PC compatible program where calculations will be done automatically. The method for deriving the analytic expressions is described in the APPENDIX *AFI Computer Algorithms for Power Density Curves.*

The number of relative power curves was restricted to 24 (2 x 3 x 4) by classifying the antenna and near-field parameters as listed in TABLE 3-2 on page 3-25.

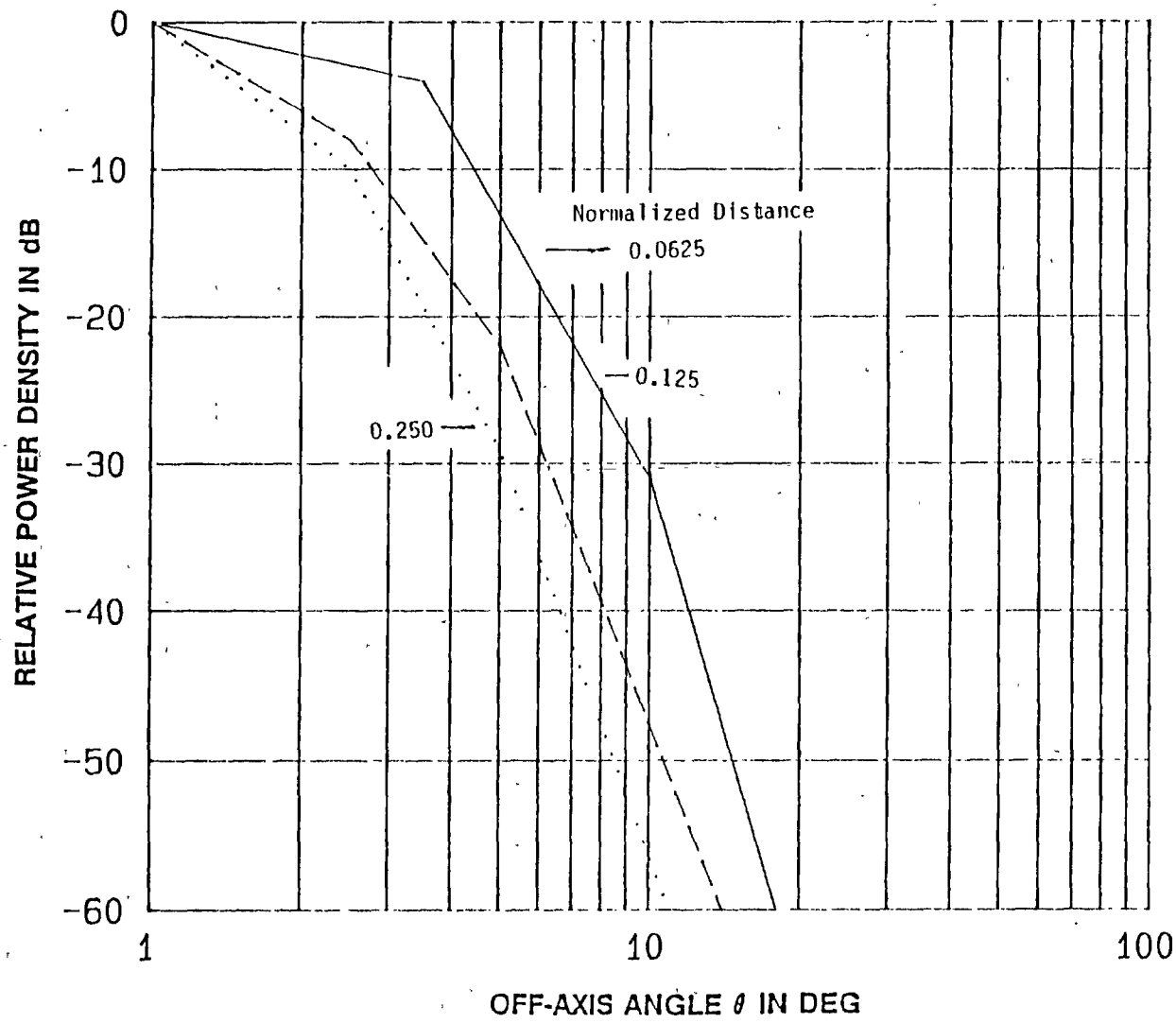

Figure 3-8a. Relative power density vs mainbeam off-axis angle. n = 2, D = 30λ, based on data from Ref. 13.

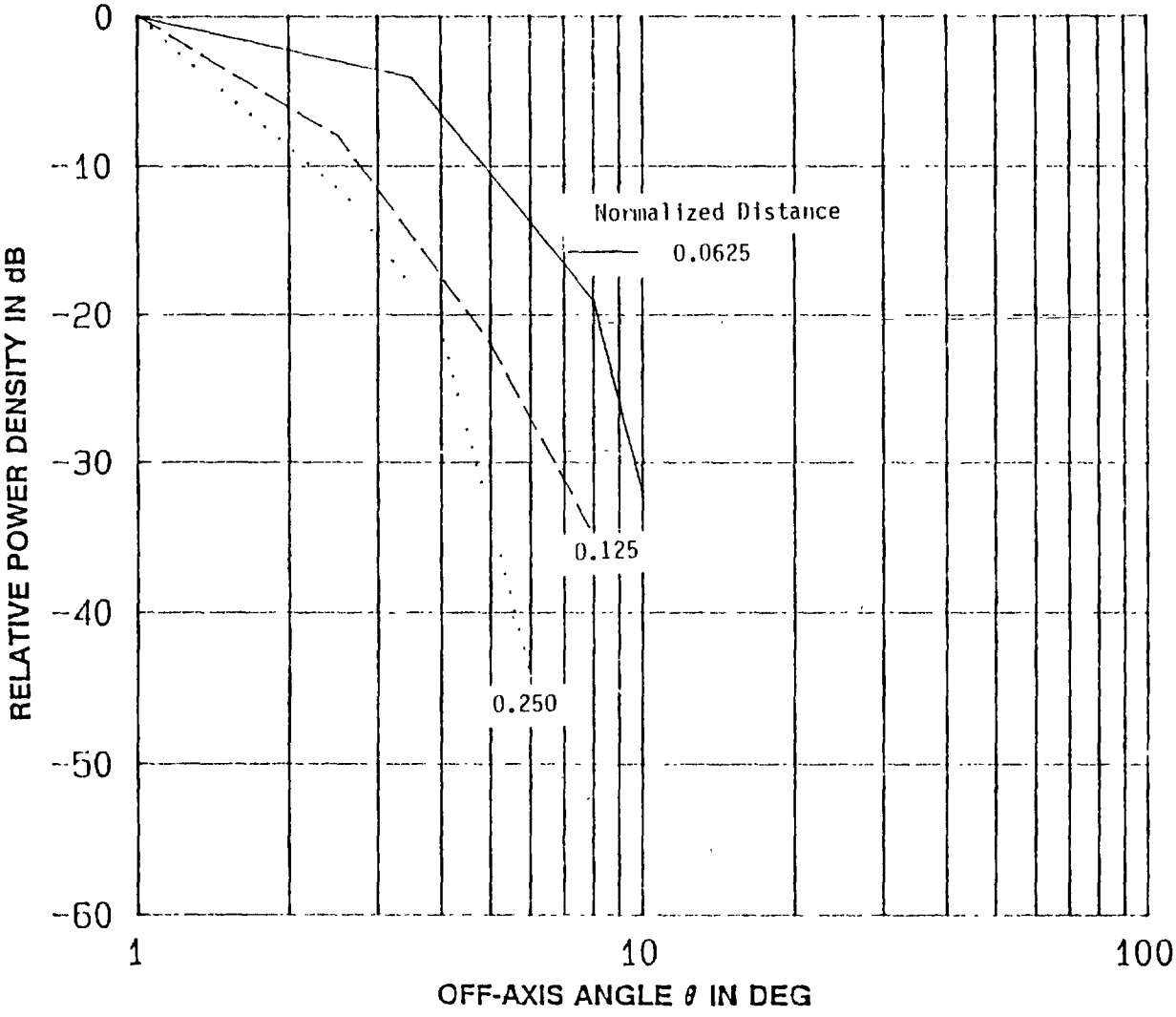

Figure 3-8b. Relative power density vs mainbeam off-axis angle. n = 2, D = 30λ, -20 dB pedestal. Data from Ref. 13.

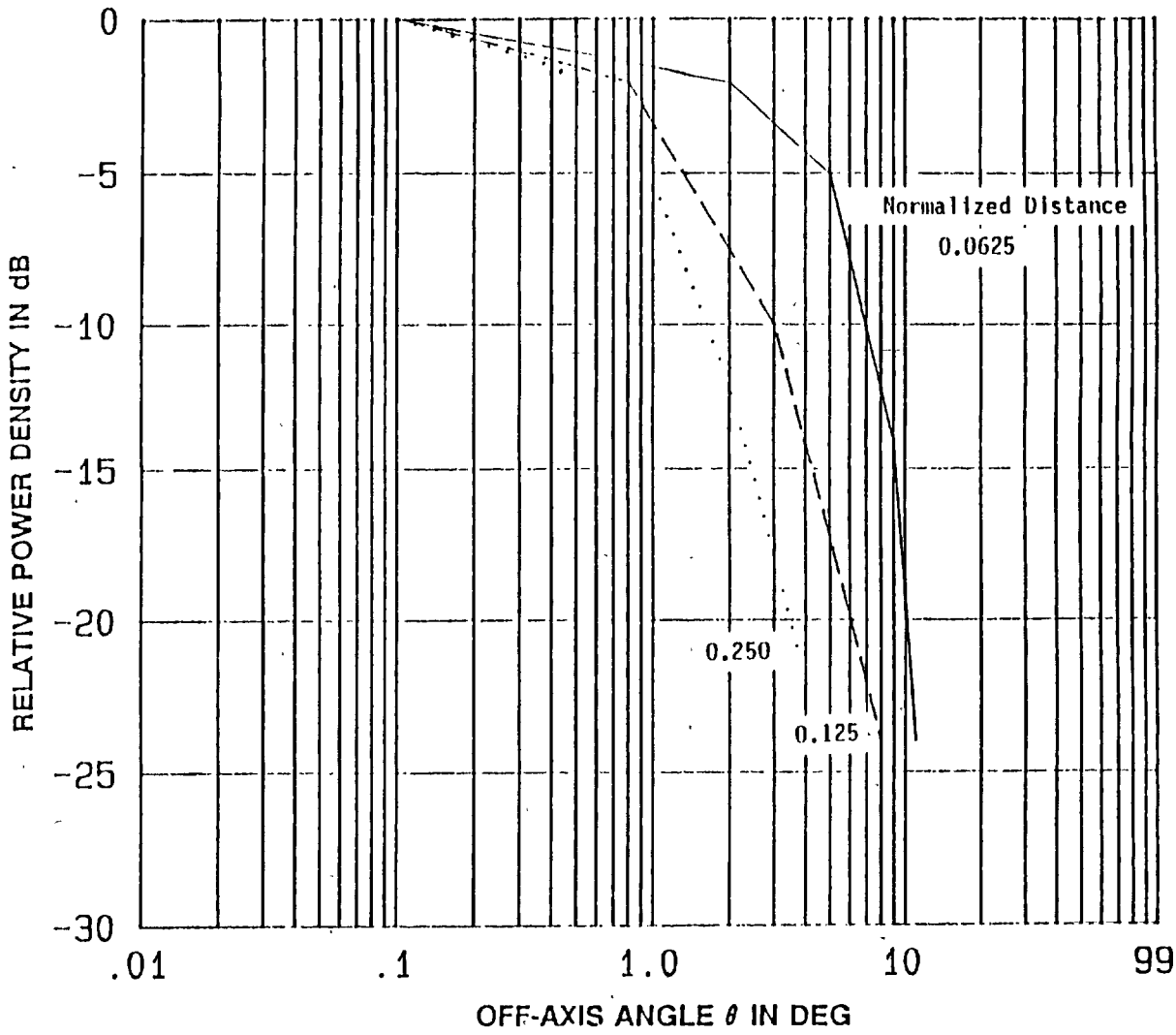

Figure 3-9a. Relative power density vs mainbeam off-axis angle. n = 0, D = 30λ, based on data from Ref. 14.

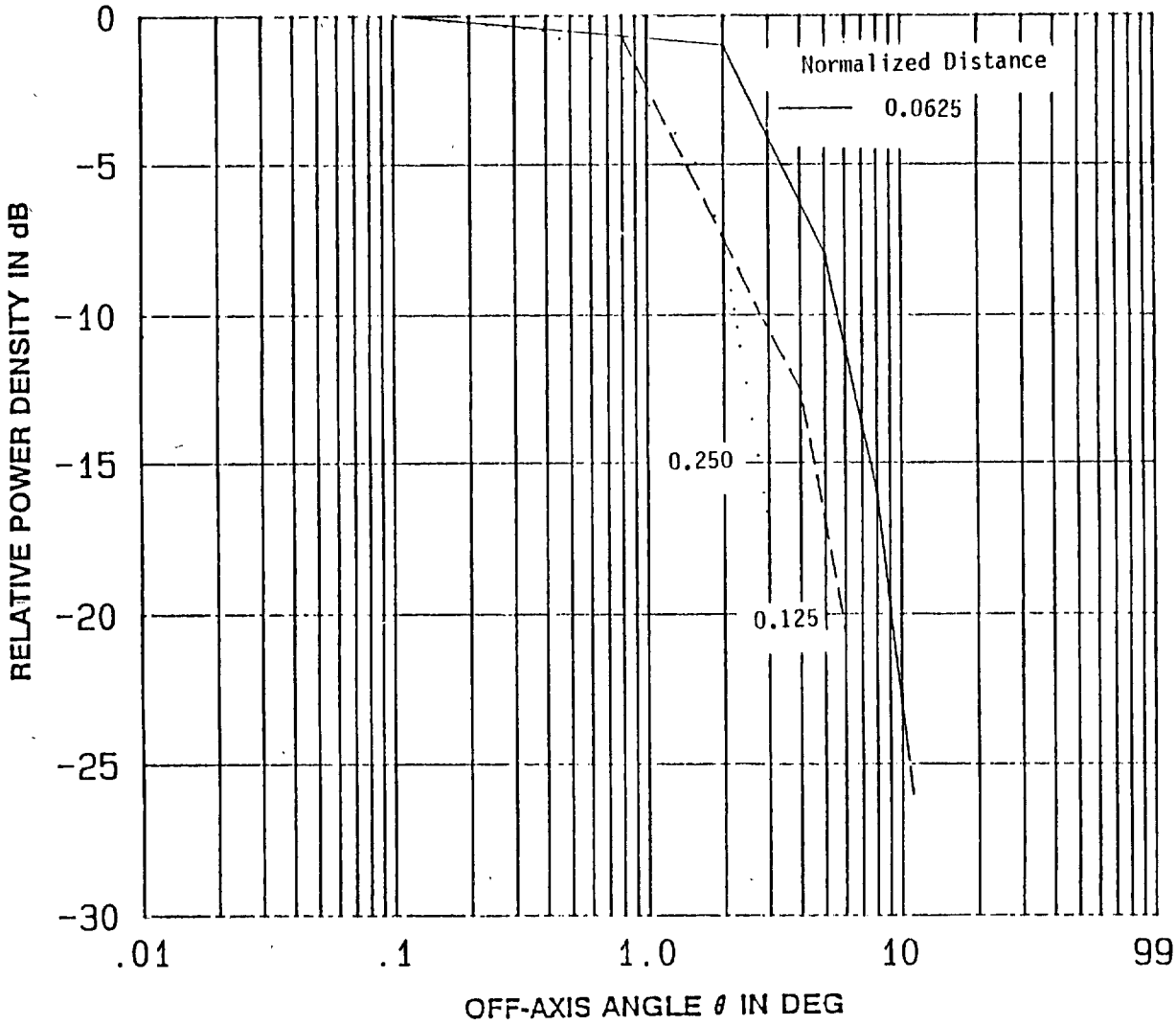

Figure 3-9b. Relative power density vs mainbeam off-axis angle. n = 1, D = 30λ, based on data from **Ref. 14.**

TABLE 3-2

PARAMETERS OF THE POWER DENSITY CURVES

Parameter	Categories
D/λ ratio	$D/\lambda < 30$
	$D/\lambda \geq 30$
Aperture taper n	$n < 0.5$
	$0.5 \leq n < 1.5$
	$1.5 \leq n < 3.5$
Normalized distance p	$0.07 < p \leq 0.1$
	$0.1 < p \leq 0.2$
	$0.2 < p \leq 0.5$
	$p > 0.5$

If the four distances are grouped together on one chart, we obtain the six charts (2 x 3) of the procedural relative power curves (Figures 3-10a through 3-10f). Very close distances ($p \leq 0.07$) are omitted because of difficulty in assessing the rapid changes in the sidelobe levels including deep bifurcation of the mainlobe(see Figure 3-3). At the other extreme, for $p > 0.5$, the sidelobes are well-behaved and tend toward far-field conditions.

To arrive at the figures themselves, a worst case viewpoint for radiation hazard assessment was adopted.

Some points worth noting are:

1. Following common procedure, all curves begin at zero dB gain and are normalized to the on-axis power density in a specified distance interval.

2. Flattening of the mainlobe at close distance and small off-axis angle is approximated by a flat or very shallow line segment.

3. The power density at angles outside of a curve is assumed to be no greater than the lowest value on the curve. This will generally give a high (therefore worse case) estimate for radiation hazard purposes.

The preparation of Figures 3-10a through 3-10f, leads to a formal procedure for calculating the off-axis near-field power density of a parabolic dish.

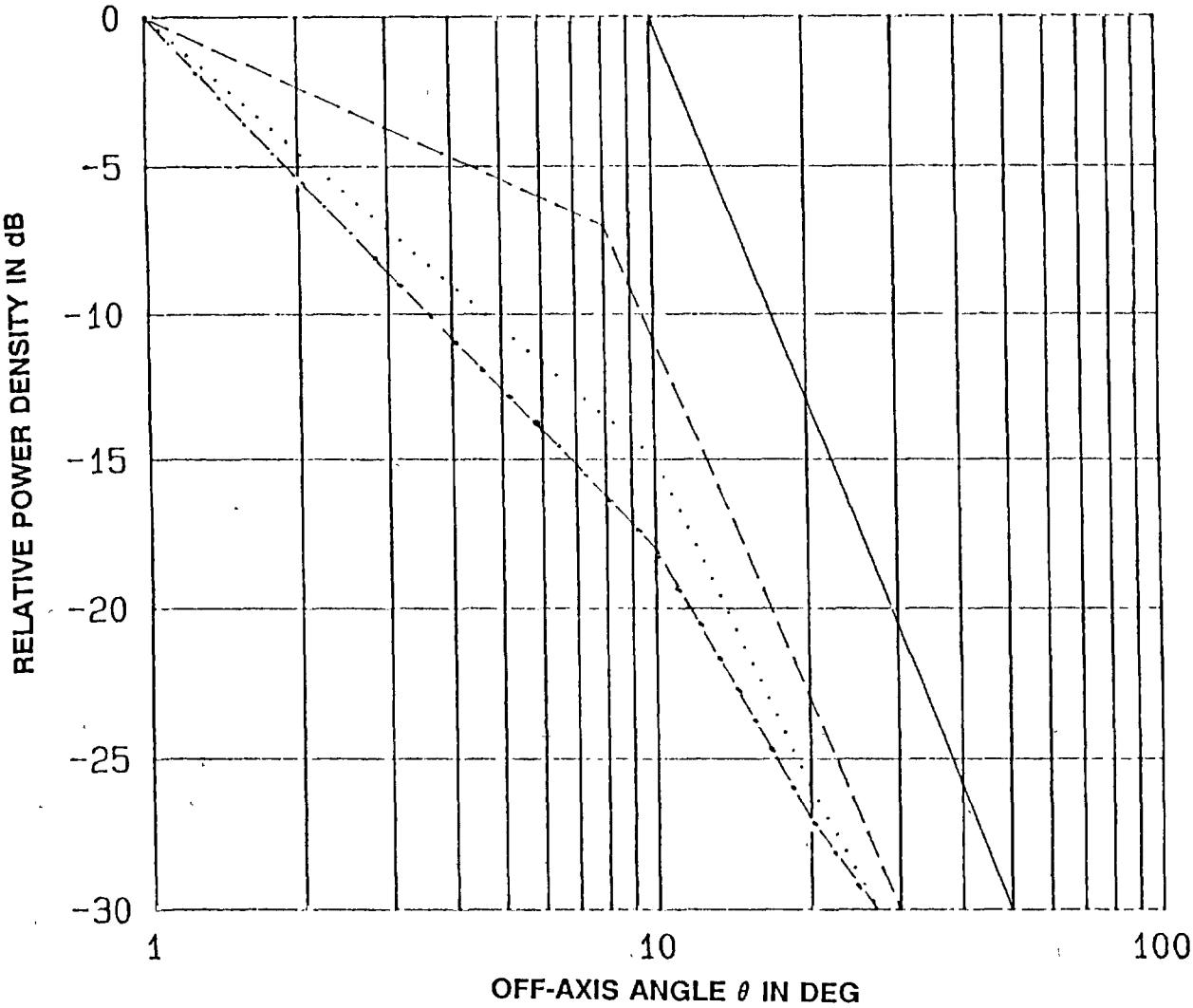

Figure 3-10a. RELATIVE POWER DENSITY CURVES
$D/\lambda < 30$, $n < 0.5$

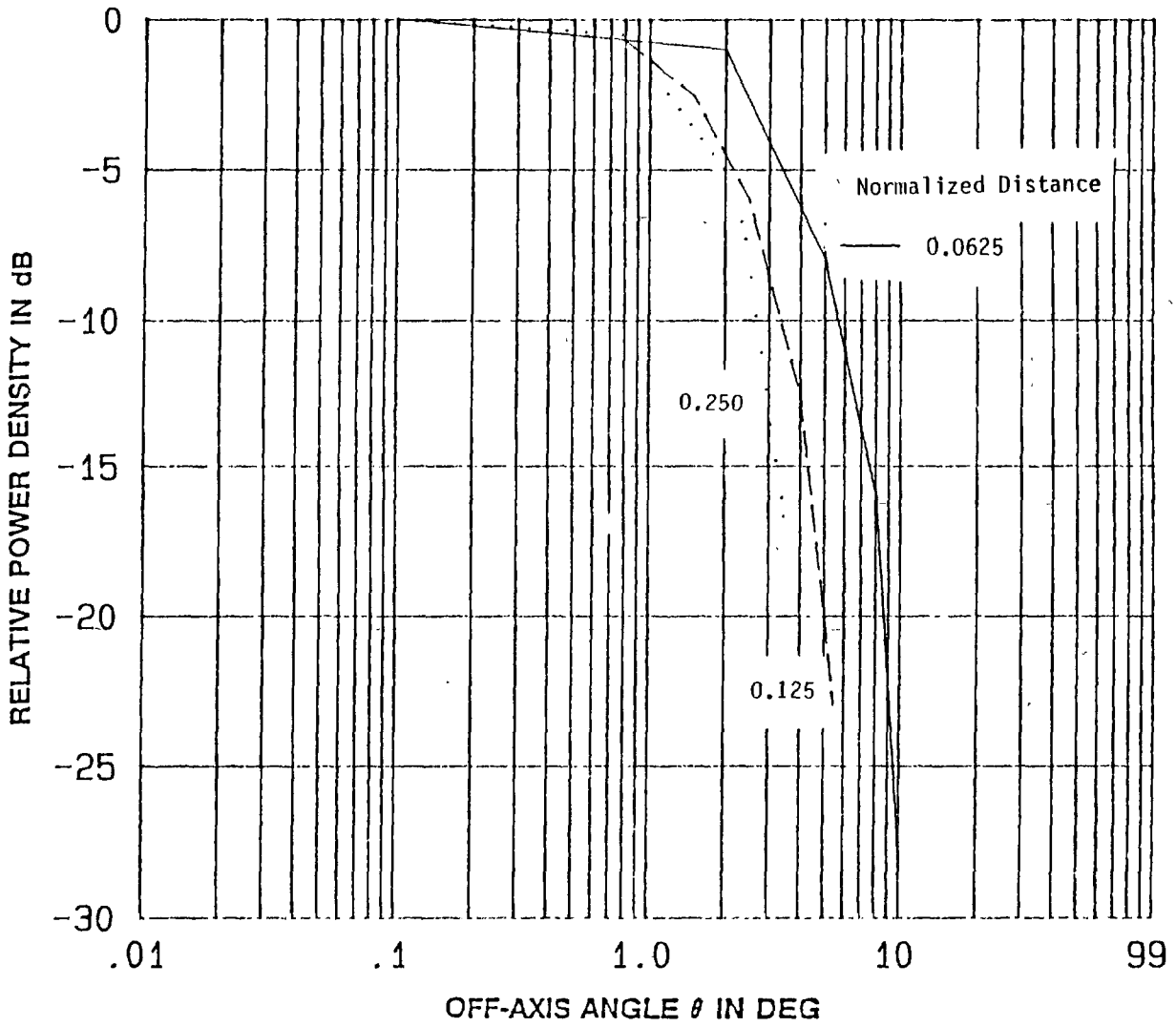

Figure 3-9c. Relative power density vs mainbeam off-axis angle. n = 2, D = 30λ, based on data from **Ref. 14.**

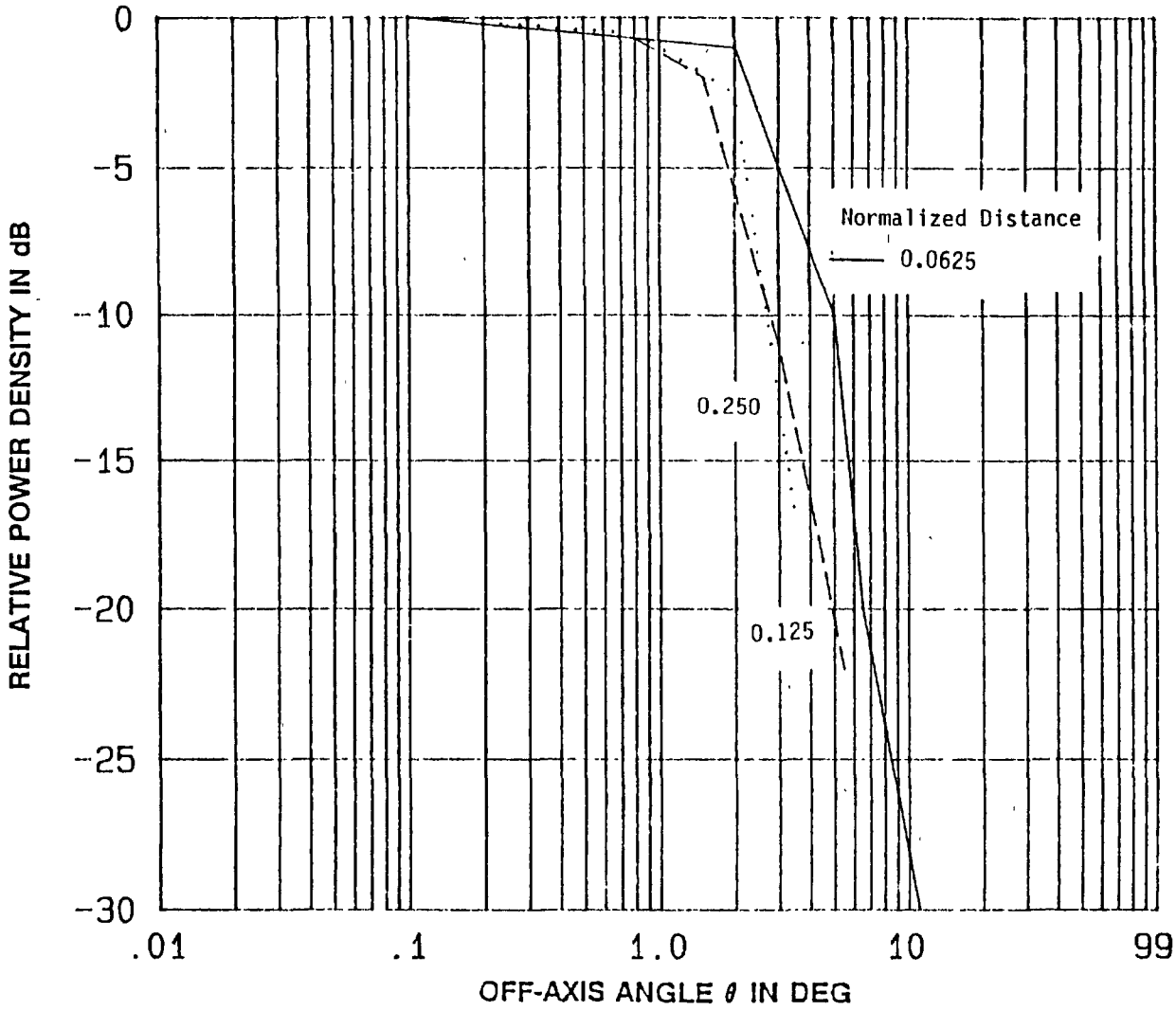

Figure 3-9d. Relative power density vs mainbeam off-axis angle. $n = 3$, $D = 30\lambda$, based on data from Ref. 14.

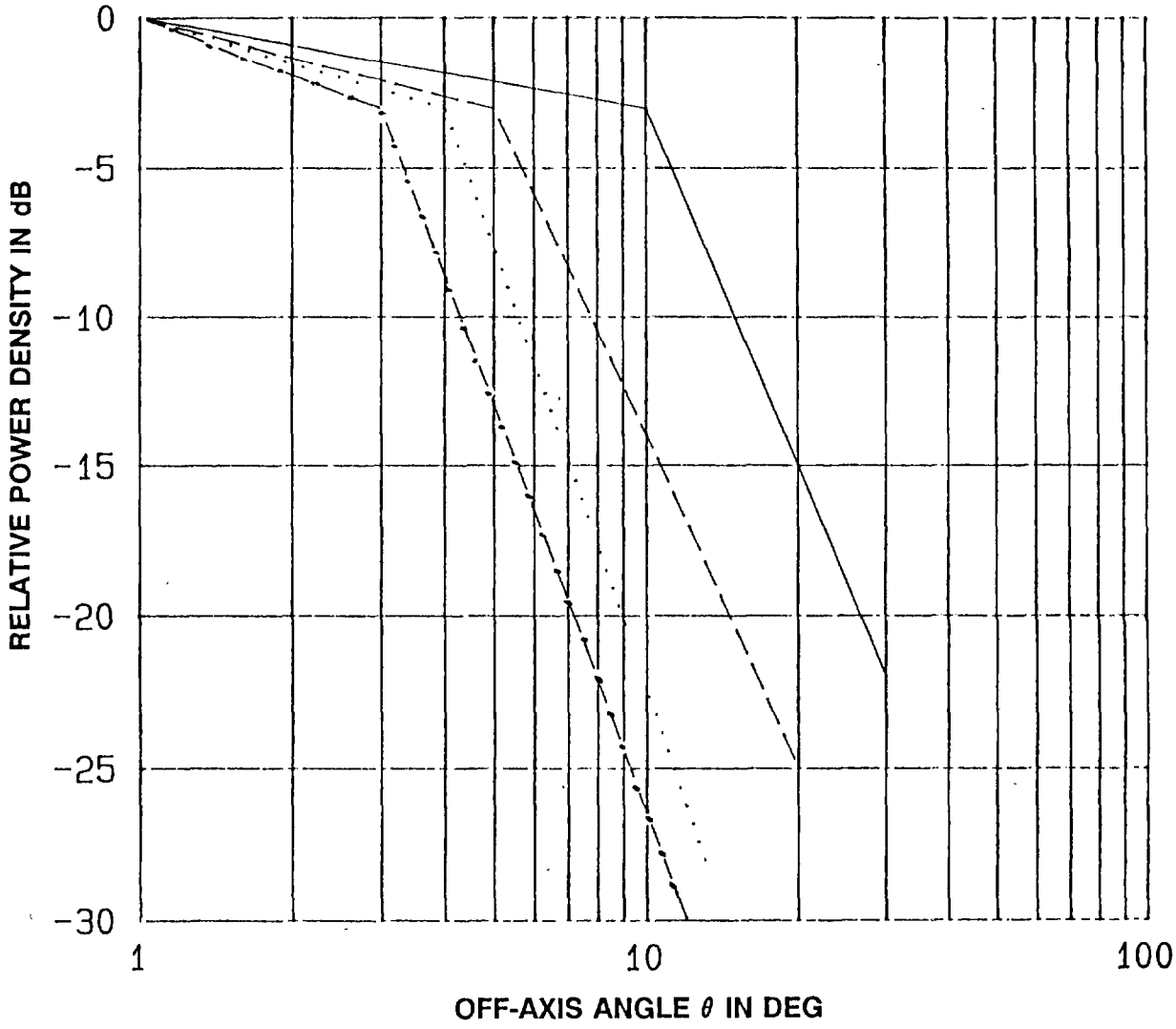

Figure 3-10b. RELATIVE POWER DENSITY CURVES
$D/\lambda < 30$, $0.5 \leq n < 1.5$

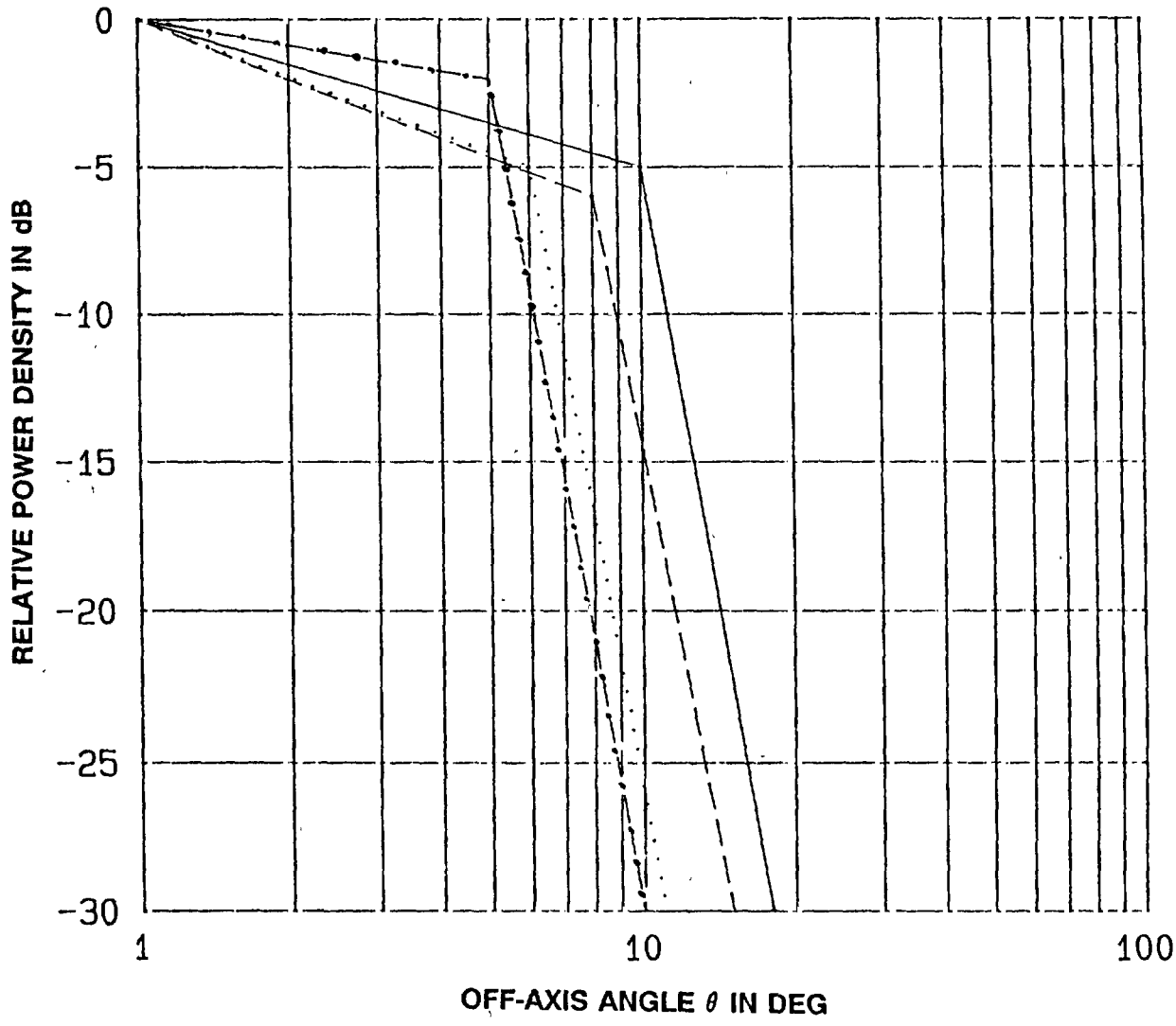

Figure 3-10c. RELATIVE POWER DENSITY CURVES
$D/\lambda < 30, \quad 1.5 \leq n < 3.5$

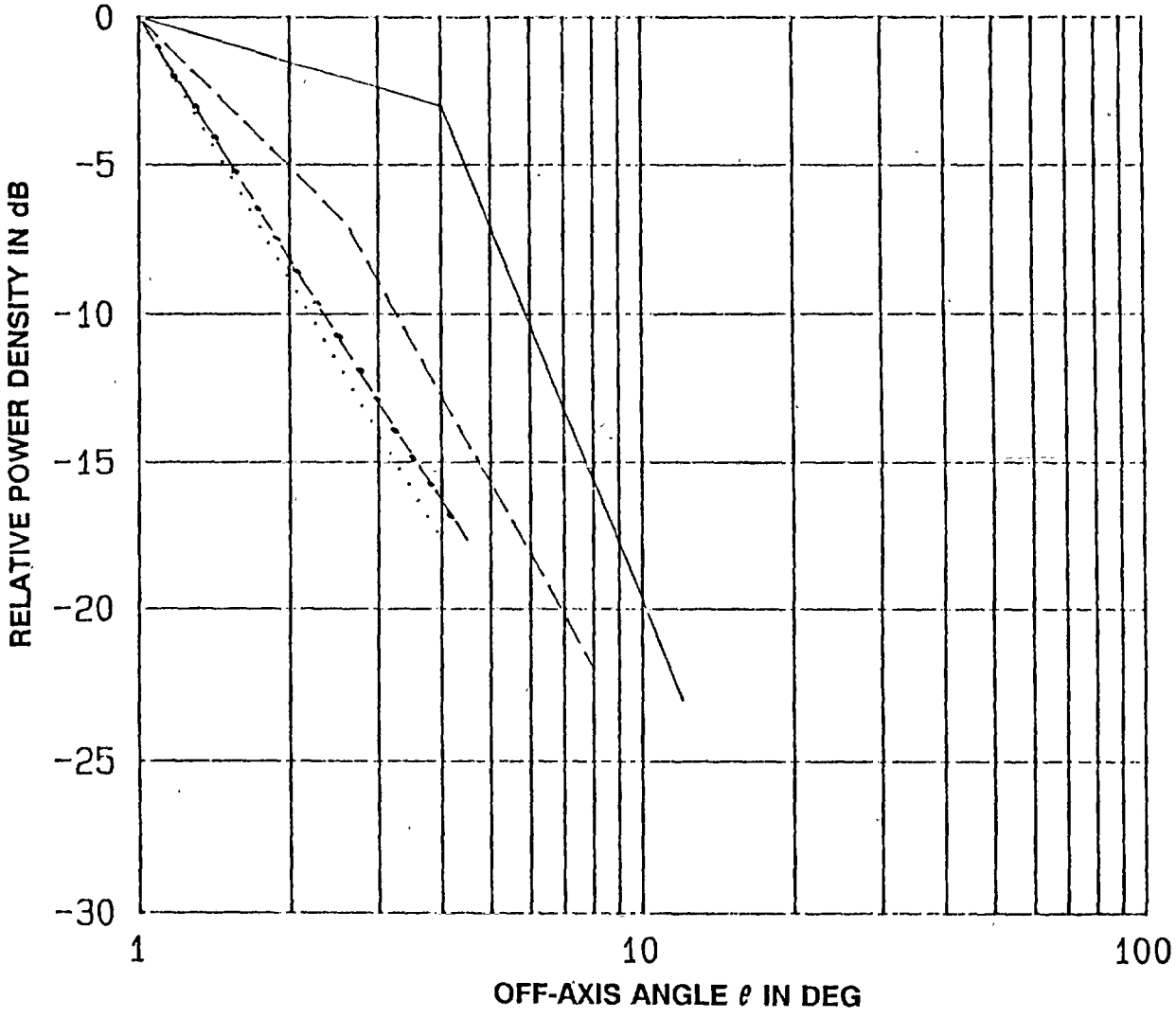

Figure 3-10d. RELATIVE POWER DENSITY CURVES
$D/\lambda \geq 30$, $n < 0.5$

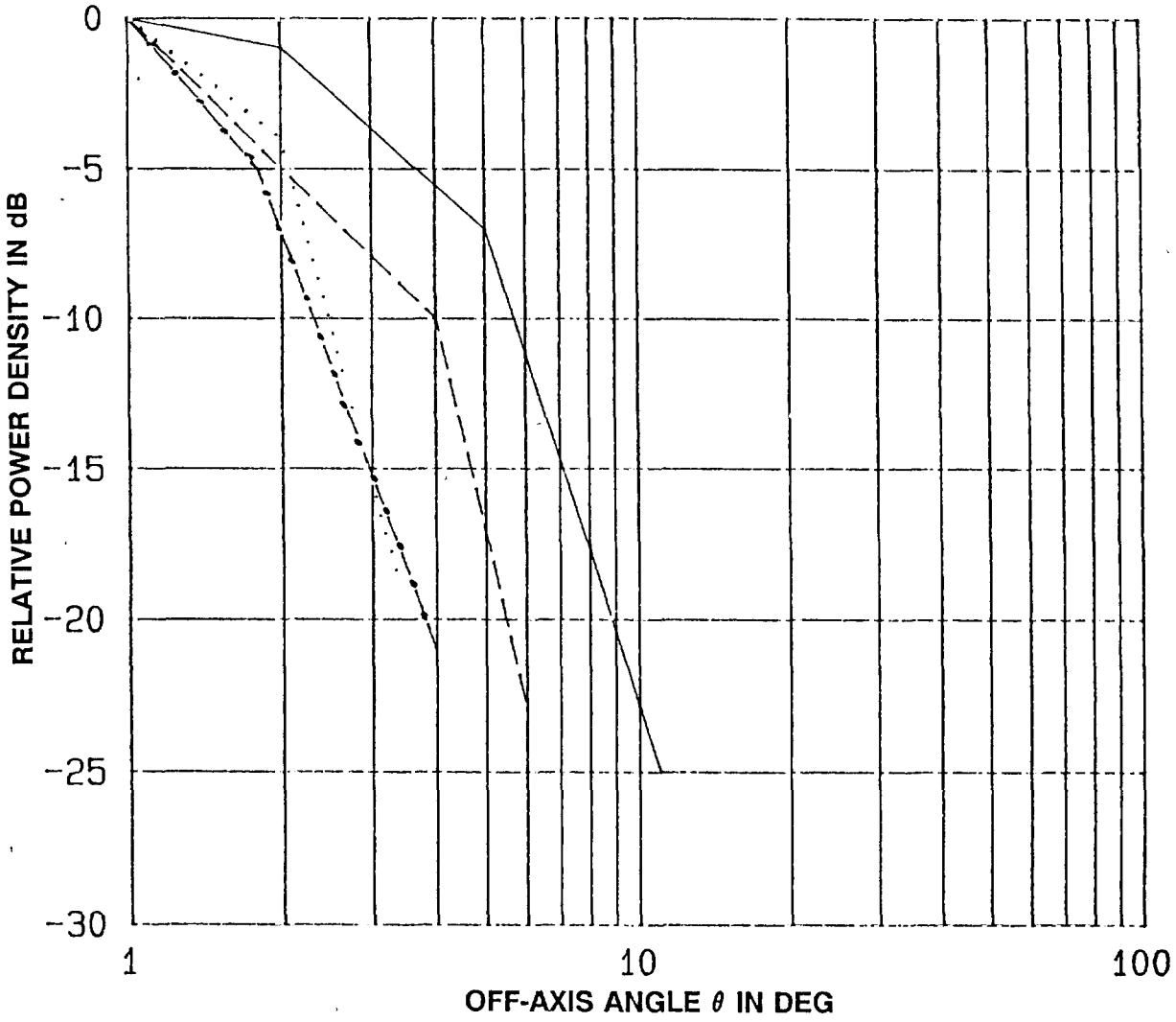

Figure 3-10e. RELATIVE POWER DENSITY CURVES
$D/\lambda \geq 30$, $0.5 \leq n < 1.5$

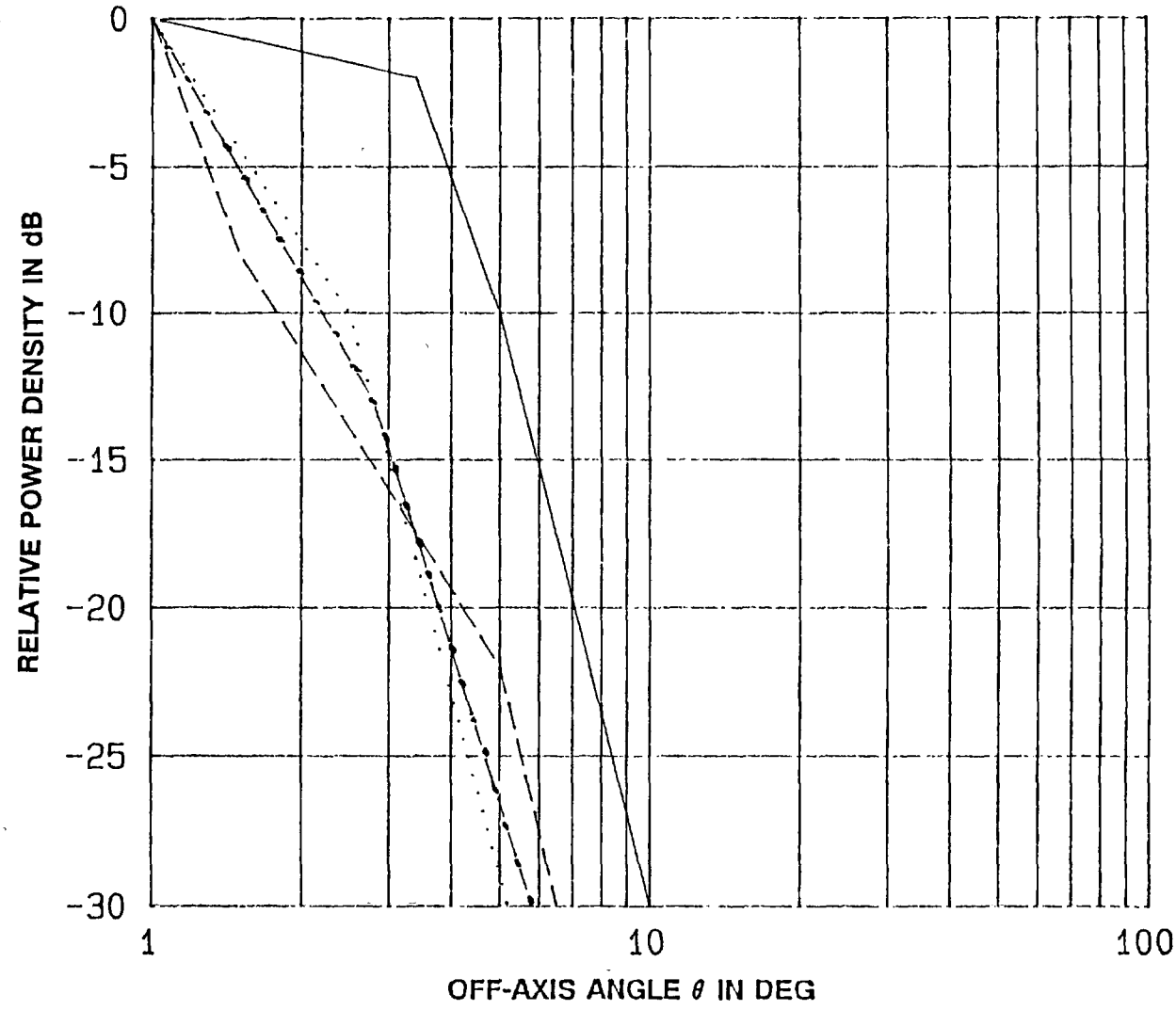

Figure 3-10f. RELATIVE POWER DENSITY CURVES
$D/\lambda \geq 30$, $1.5 \leq n < 3.5$

SECTION 4

PROCEDURE FOR CALCULATING THE POWER DENSITY OF A PARABOLIC CIRCULAR REFLECTOR ANTENNA

INTRODUCTION

The procedure closely follows those developed for the mainbeam on-axis calculations of antennas by NTIA (Refs. 2 and 3). Some familiarity with obtaining the on-axis power density of parabolic circular reflector antennas is helpful, although the following procedure will point to where and how this may be done. Limitations for off-axis and on-axis analyses are identical and are detailed in Refs. 2, 3, and 5. In particular, the effect of the feed, struts, and other structural elements has not been taken into account.

GENERAL PROCEDURE

STEP 1. Determine the on-axis power density for a circular aperture antenna at the desired distance.

This is done by manual calculations from the example in Ref. 2, pages 4-38 and 4-39, or by selecting the circular aperture antenna option in the AFI IBM-PC program (Ref. 4).

Input quantities required:	Units
* Distance from dish aperture along mainlobe axis	meters
Frequency of emission	GHz
Average input power to antenna	Watts
Antenna gain for on-axis mainlobe	dBi
Half-power beamwidth	degrees
** Diameter of dish	meters
** First sidelobe level below mainlobe	minus dB

* If the off-axis angle θ and its corresponding distance h (the hypotenuse) are given, the on-axis distance d may be found by the definition

$$d = h \cos \theta \qquad (4\text{-}1)$$

** This quantity is a useful check on consistency between given values for frequency, dish diameter, and half-power beamwidth. In Table 3-1, these should agree for any aperture taper n.

STEP 2. Find the input parameters for the off-axis procedure.

a. D/λ ratio

The D/λ ratio is available as an intermediate computation in the manual calculations of Step 1. For AFI program users, the ratio is easily obtained from Table 3-1 where the half-power beamwidth (in radians) multiplied by a factor gives the D/λ ratio.

b. Aperture taper n

The aperture taper n is also part of the manual computations. AFI users can find this parameter from Table 3-1 after getting the D/λ ratio from the half-power beamwidth.

c. Normalized distance p

The normalized distance p, a part of the manual computations, can be found by AFI users from the following proportional relationship obtained from Equation 3-3:

$$p = d/(2D^2/\lambda) \qquad (4\text{-}2)$$

where d = distance along the mainlobe axis

STEP 3. Look up the relative power density "correction."

The parameters obtained in Step 2 will point to one of the 24 curves of Figures 3-10a through 3-10f, and for the given off-axis angle θ, a "correction" to the on-axis power density.

STEP 4. Combine the on-axis power density and the "correction."

The results of Step 1 and Step 4 are multiplied to give the final answer. Care must be taken that the results are for the same on-axis distance. This is particularly important close to the antenna where the sidelobe levels are relatively high.

WORKED EXAMPLE

Step-by-step procedure:

The on-axis example from Ref. 2 (pages 4-38 and 4-39) with its intermediate and final calculations will be carried through for an off-axis analysis. The input data are:

Distance from dish aperture along the mainlobe axis	40 m
Frequency of Emission	3 GHz
Average input power to antenna	1 W
Antenna gain for on-axis mainlobe	38 dBi
Half-power beamwidth	2.25 degs
First sidelobe level below mainlobe	−30.6 dB
note: Dish diameter D is not needed as an input	

The power density at 40 m was found to be 0.0435 mW/cm^2. The intermediate steps in computation yielded:

D/λ ratio	37.7
Aperture taper n	2.0
Normalized distance p	0.14

Figure 3-9f corresponds to the values above. For 4 degrees off-axis the relative power density is −19 dB or 0.0126. Multiplying this number by 0.0435 yields the final answer 0.000548 mW/cm^2.

Comments on example:

This is an example of a relatively narrowbeam antenna. The half-power beamwidth of 2.25 degrees agrees closely with the corresponding point of 1.125 degrees on the far-field $p < 0.5$ curve; i.e. relative power density is about minus 3 dB. Moving only 6 degrees off-axis drops the power level well below −30 dB.

Contrast this antenna with one of opposite characteristics; e.g. a small dish ($D/\lambda < 30$) with uniform aperture illumination (n = 0). Figure 3-8a corresponding to such an antenna shows a drop of only −14 dB six degrees off-axis. For close distances (solid line curve) the power density does not change until the 10-degree angle is exceeded.

APPENDIX

AFI COMPUTER ALGORITHMS FOR POWER DENSITY CURVES

The purpose of this appendix is to outline a simple method whereby the relative power density curves of Figures 3-10a through 3-10f can be replaced by mathematical algorithms in the AFI computer program. This would avoid mistakes in setting up multidimensional tables of lookup numbers needed to represent the 24 power density curves. The pathway to a particular set of algorithms is based on TABLE 3-2. All pathways are depicted in Figure A-1.

The far-field power density for aperture antennas are often expressible as a simple, monotonically decreasing function. For example, the CCIR recommends that the gain G of the sidelobe peaks of large satcom earth station antennas should not exceed[15]

$$G = 32 - 25 \log \theta \qquad \text{dBi} \qquad 1 < \theta < 48 \text{ degs}$$

A normalized power density curve of Figures 3-10a through 3-10b is also made up of linear log segments, each of which can be represented by a general equation:

$$G = A + B \log \theta \qquad \theta_1 < \theta < \theta_2 \qquad \text{(A-1)}$$

where A and B are constants, and 1 and 2 denote the range of θ.

Figure A-2 is a graphical representation of Equation A-1. An expression linking the relative power density to any angle between θ_1 and θ_2 will now be derived.

For the line segment between points 1 and 2 in Figure A-2, we can set up the following proportional equivalents between slopes:

$$\frac{G_i - G_1}{\log (\theta_i / \theta_1)} = \frac{G_2 - G_1}{\log (\theta_2 / \theta_1)}$$

---

[15] CCIR, *Handbook Satellite Communications*, International Telecommunication Union, Geneva, Switzerland, 1988.

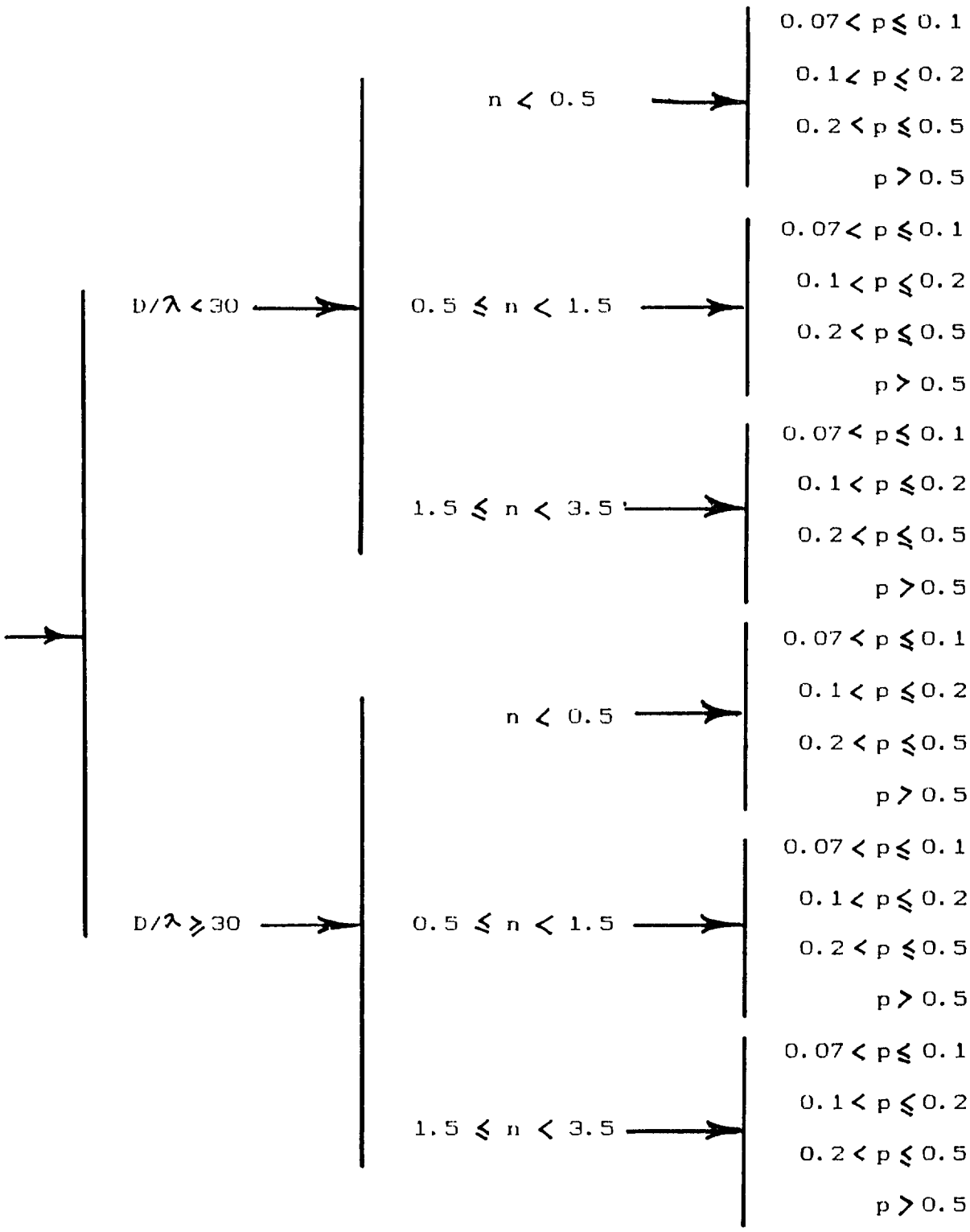

Figure A-1. Pathway for selection of a normalized power density curve based on TABLE 3-2.

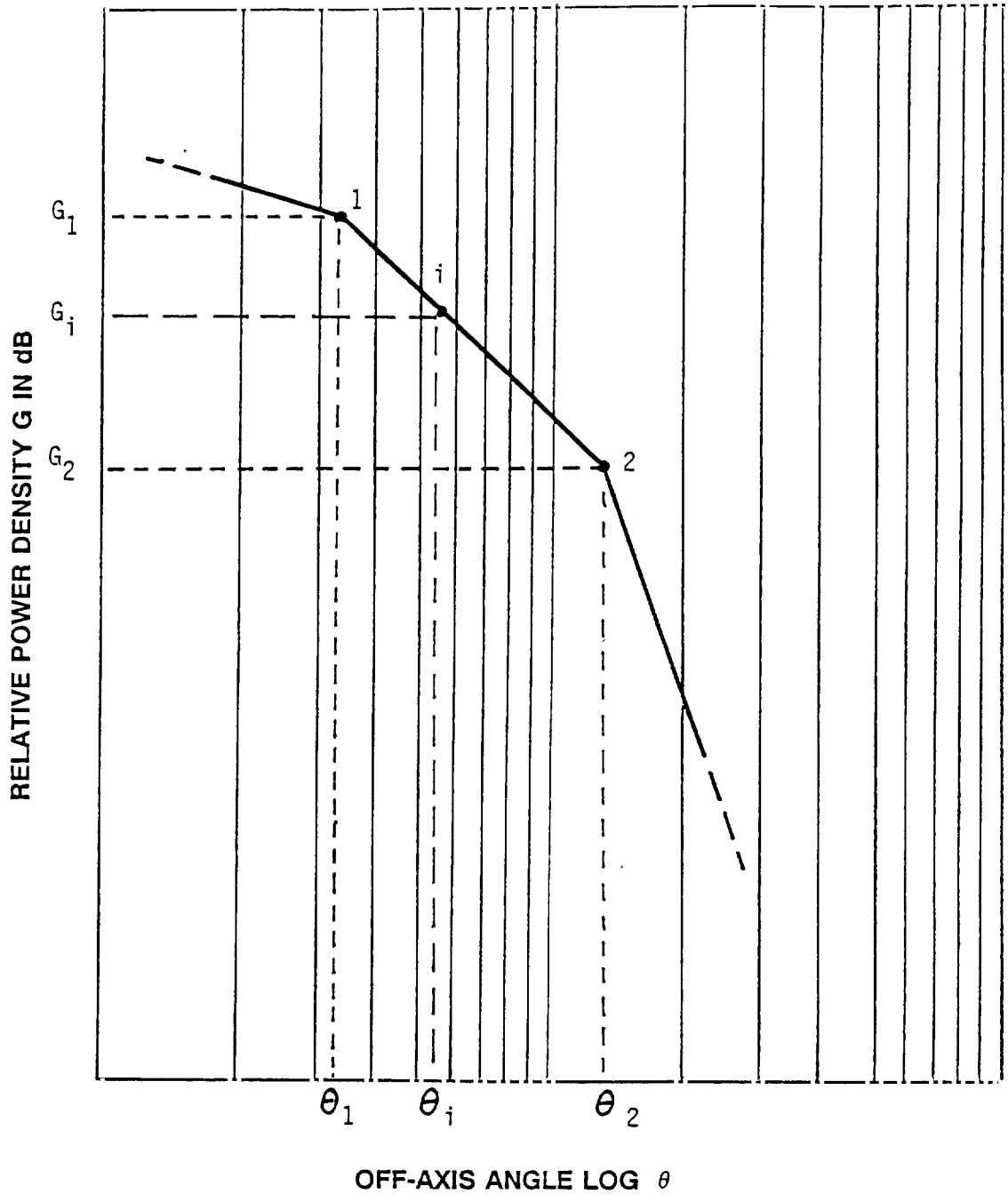

Figure A-2. Generalized relative power density curve.

where G_i is the density for a given angle θ_i.

Solving for G_i, we obtain:

$$G_i = G_1 + (G_2 - G_1) \frac{\log (\theta_i / \theta_1)}{\log (\theta_2 / \theta_1)} \qquad \theta_1 \leq \theta \leq \theta_2 \qquad \text{(A-2)}$$

Equation A-2 can be used with any two pairs of (θ, G) to get a value for G at an intermediate point. Validity of the equation can be checked with Figures 3-10a through 3-10f. For example, substituting endpoint values for the middle section of the solid-line curve in Figure 3-10e, and θ_i = 4.0 degrees:

$$G_i = -1.0 + [-7.0 - (-1.0)] \frac{\log (4.0/2.0)}{\log (5.0/2.0)} \qquad 2.0 \leq \theta \leq 5.0$$
$$= -5.5 \text{ dB}$$

From the curve itself, we see that the answer is correct.

In the AFI3 program, the sequence of steps for obtaining the off-axis power density would be:

1. Determine the on-axis power density from the present AFI program.

2. Reach a table of stored (θ, G) for a curve by tracing the pathway of Figure A-1. D/λ, n, and p are from step 1.

3. Substitute the off-axis angle θ and a pair of stored values in Equation A-2 to get G_i.

4. Multiply the on-axis power density of step 1 by G_i.

LIST OF REFERENCES

1. NTIA, *Manual of Regulations and Procedures for Federal Radio Frequency Management*, U.S. Department of Commerce, National Telecommunications and Information Administration, Washington, D.C., Revised May 1989.

2. Farrar, A. and Chang E., *Procedures for Calculating Field Intensities of Antennas*, NTIA Report TM-87-129, U.S. Department of Commerce, September 1987.

3. Kobayashi, H. K., *Procedures for Calculating Field Intensities of Antennas: Phase II*, NTIA Report TM-88-135, U.S. Department of Commerce, September 1988.

4. American National Standards Institute, *Safety Levels with Respect to Human Exposure to Radio Frequency Electromagnetic Fields, 300 kHz to 100 GHz*, Report No. ANSI C95.1-1982, Institute of Electrical and Electronic Engineers, Inc., New York, NY, 1982.

5. Calhoon, E. and Kobayashi, H. K., *Documentation for the Antenna Field Intensity Program Version 2 (AF12)*, NTIA/CSD, Annapolis, MD, not yet published.

6. Mumford, W. W., *Some Technical Aspects of Microwave Radiation Hazards*, IRE (IEEE) Proceedings, Vol. 49, no. 2, pp. 427-447, February 1961.

7. National Council on Radiation Protection and Measurements, *Biological Effects and Exposure Criteria for Radio Frequency Electromagnetic Fields*, page 274, NCRP Report No. 86, National Council on Radiation Protection and Measurements, Bethesda, MD, 1986.

8. Silver, S. (Editor), *Microwave Antenna Theory and Design*, pages 192-195, McGraw-Hill, Inc., New York, NY, 1949.

9. Bickmore, R. W. and Hansen, R. C., *Antenna Power Densities in the Fresnel Region*, IRE (IEEE) Proceedings, pp. 2119-2120, December 1959.

10. Skolnik, M. I. (Editor), *Radar Handbook*, pages 9-20 to 9-24, McGraw-Hill, Inc., New York, NY, 1970.

11. Farrar, A. and Adams, A. T., *An Improved Model for Calculating the Near Field Power Densities of Aperture Antennas*, IEEE International Symposium on Electromagnetic Compatibility, pp. 134-137, 1980.

LIST OF REFERENCES
(continued)

12. Lewis and Newell, *An Efficient and Accurate Method for Calculating and Representing Power Density in the Near-Zone of Microwave Antennas*, NBSIR 85-3036, December 1985.

13. Hansen, R. C. and L. L. Bailin, *A New Method of Near Field Analysis*, IRE (IEEE) Transactions on Antennas and Propagation, pp. S458-A467, December 1959.

14. Maddocks, H. C. (Editor), *ECAC Antenna Engineering Handbook*, pages 5-65 to 5-74, IIT Research Institute, ECAC-HDBK-79-05d1, revised October 1985.

15. CCIR, *Handbook Satellite Communications*, International Telecommunication Union, Geneva, Switzerland, 1988.

FORM NTIA-29
(4-80)

U S DEPARTMENT OF COMMERCE
NAT L TELECOMMUNICATIONS AND INFORMATION ADMINISTRATION

BIBLIOGRAPHIC DATA SHEET

	1 PUBLICATION NO NTIA TM-90-145	2 Gov't Accession No
3 Recipient's Accession No		

4 TITLE AND SUBTITLE
PROCEDURE FOR CALCULATING THE POWER DENSITY OF A PARABOLIC CIRCULAR REFLECTOR ANTENNA

5 Publication Date
FEBRUARY 1990

6 Performing Organization Code
NTIA/OSM/SEAD

7 AUTHOR(S)
Herbert K. Kobayashi

8 PERFORMING ORGANIZATION NAME AND ADDRESS
National Telecommunications and
Information Administration
179 Admiral Cochrane Drive
Annapolis, Maryland 21401

9 Project/Task/Work Unit No
9010171

10 Contract/Grant No

11 Sponsoring Organization Name and Address
U.S. Department of Commerce/NTIA
179 Admiral Cochrane Drive
Annapolis, Maryland 21401

12 Type of Report and Period Covered
TECHNICAL MEMORANDUM

13

14 SUPPLEMENTARY NOTES

15 ABSTRACT *(A 200-word or less factual summary of most significant information If document includes a significant bibliography or literature survey, mention it here)*

This technical report details a procedure for calculating the mainbeam off-axis power density in the near- and far-field of a parabolic circular reflector antenna. In this report, the on-axis procedures of NTIA TM-87-129 and its IBM-PC compatible Antenna Field Intensity (AFI) program are extended to off-axis analysis. Like its predecessors, it is intended for general use in system planning and evaluation and gives a worst-case estimate for radiation hazard assessment.

This procedure starts with the on-axis power density at a given distance obtained from the TM-88-129 report or AFI PC program. This is multiplied by the normalized near-field power density for the chosen off-axis angle to give a final answer.

The simple log-function form of the normalized curves lends itself to inclusion in the automated AFI program as a computer algorithm.

The method chosen for developing the procedure is general and may be applied to other directive antennas provided sufficient near-field off-axis data are available.

16 Key Words *(Alphabetical order, separated by semicolons)*
Antenna Field Intensity (AFI) Program; Near-Field Off-axis Power Density; On-axis Field Intensity; Parabolic Reflector (Circular)

17. AVAILABILITY STATEMENT ☒ UNLIMITED ☐ FOR OFFICIAL DISTR'BUTION	18 Security Class *(This report)* UNCLASSIFIED 19 Security Class *(This page)* UNCLASSIFIED	20 Number of pages 52 21 Price

☆ U S Government Printing Office 1980—678 495/529